DEPARTMENT OF THE ARMY CORPS OF ENGINEERS

BEACH EROSION BOARD

OFFICE OF THE CHIEF OF ENGINEERS

TURBULENT FLOW NEAR AN OSCILLATING WALL

TECHNICAL MEMORANDUM NO. 97

TURBULENT FLOW NEAR AN OSCILLATING WALL

TECHNICAL MEMORANDUM NO. 97
BEACH EROSION BOARD
CORPS OF ENGINEERS

JULY 1957

FOREWORD

Any theoretical description of sediment movement under wave action must necessarily start with a definition of the oscillating flow near the bottom due to the surface waves. Although much theoretical and experimental work has been done by others on defining the motion of water near the bottom in unidirectional flow such as exists in rivers and flumes, little work has been done on defining the comparable action in oscillating flow accompanying wave action. This paper presents the result of recent theoretical and experimental work done to define these bottom flow conditions under wave action. The flow conditions are described mathematically and the values of certain coefficients are defined from the experimental results using an oscillating bed.

The present paper confines itself to flow conditions with a smooth bottom and to waves of low amplitude in deep water.

The report was prepared at the Wave Research Laboratory of the Institute of Engineering Research at the University of California in Berkeley in pursuance of contract DA-49-055-eng-17 with the Beach Erosion Board, which provides in part for the study of the mechanics of sediment movement under wave action. The author of this report, George Kalkanis, is a Research Engineer at that institution.

This report is published under authority of Public Law 166, 79th Congress, approved July 31, 1945.

TABLE OF CONTENTS

LIST OF FIGURES

LIST OF SYMBOLS

A, A_1	Functions of z, denoting the decay of the amplitude with increasing distance from the wall.
A_o	Area of the central electrode.
a	$\sqrt{c(c-1)}$
a_1	$\sqrt{c(c+1)}$
a'	Length of semi-amplitude at any depth.
a'_b	Semi-amplitude of the oscillation at the bottom.
a_o	Effective area of the diaphragm.
B, B_1	Functions of z denoting the phase shift.
B_2	T_1/T_3
c	Exponent.
c^o	Velocity of transversely propagating wave.
C_o	Capacitance of the instrument.
d	Depth of water.
d'	$2a'_b$
D	Effective diameter of horizontal tube.
D_1	Diameter of vertical tube.
D_2	Effective diameter of diaphragm.
d_o	Distance between the central electrode and the diaphragm.
E	Young's modulus.
H	Surface wave height.
K, K_1	Constants determined experimentally.
k	Dielectric constant.
L	Length of surface wave.
ℓ	Adjustable amplitude of plunger motion
ℓ'	Mixing length.
N_R	Reynold's number.
P	Pressure on the diaphragm.
q	Natural frequency of the instrument.
T	Period of the oscillation.
T_o	Thickness of the diaphragm.

T_1	Kinetic energy of the diaphragm.
t	Time.
$u_{(z,t)}$	Velocity component of the main flow in the x direction.
u_o	$a'_b\omega$ maximum amplitude of the velocity.
V	Potential energy of the diaphragm.
X_c	Maximum deflection of the diaphragm.
y	Displacement of the needle of the recorder.
z	Distance from the M.W.L. or from the wall.
z_o	Distance from the wall of the reference plane.
ϵ	Eddy or mechanical viscosity.
ϵ_m	Coefficient of momentum exchange.
ϵ_v	Coefficient of vorticity exchange.
λ	Length of transversely propagated wave.
ν	Kinematic viscosity of water.
ρ	Density.
σ	Poisson's ratio.
τ	Shear stress.
ω	$\frac{2\pi}{T}$ angular velocity of wave.

TURBULENT FLOW NEAR AN OSCILLATING WALL

by
George Kalkanis
University of California, Berkeley, California

INTRODUCTION

It has been noticed long ago and it is a matter of common knowledge that sediment transport occurs near the beaches of oceans and lakes. This motion has components toward and along the coast and is attributed to the action of the waves. Moreover, recent observations reveal that a considerable amount of sediment movement occurs at localities far beyond the surf zone at depths up to sixty feet and more. An accurate estimate of the transport is very valuable to the successful handling of coastal projects. Laboratory studies have proved that the main cause of motion in this case is again the action of the surface waves.

The sand grains which constitute this transport move near or on the bottom in a similar way to the bed load in the case of unidirectional flow. Extensive studies dealing with the latter case proved the existence of a relationship between the flow near the bottom and the movement of the sediment. The modern theories of bed load motion are based on the condition of instantaneous equilibrium between the hydrodynamic and the gravitational forces acting upon the individual grains.[3][5]* It is reasonable to expect that a similar relationship should also exist in the present case where the flow is not unidirectional, but oscillatory. Our problem thus calls for the derivation of a law describing the flow near the bottom due to surface waves from which the hydrodynamic forces on the grains can be derived. Only the case of waves of small amplitude and great length in relatively deep water has been considered in the present study. Under this condition the flow within the main body of water can be described by applying the irrotational flow theory.[1]

GENERAL CONSIDERATIONS

According to the irrotational flow theory the viscous effect of the fluid can be neglected in comparison with the inertia forces. The parameters governing the flow are the amplitude and the length of the wave and the depth of the water. The water particles describe circular paths near the surface and elliptical as the depth increases. At the bottom itself the motion approaches closely a rectilinear horizontal oscillation of simple harmonic form.[1] [11]

$$u_{(z,t)} = - a'_b \omega \sin\left(\omega t - \frac{2\pi x}{L}\right) \qquad (1)$$

*Numbers in parentheses refer to references listed at the end of this paper.

The semi-orbit amplitude of the water particle motion at the bottom is

$$a'_b = \frac{1}{2} H \frac{1}{\sin h \frac{2\pi d}{L}} \qquad (1a)$$

where

H = the amplitude of the surface wave
L = the wave length
d = the depth of the water

Recalling here that only shallow waves of great length are considered it is possible to substitute for equation (1) the simpler expression

$$u = a'_b \omega \sin \omega t \qquad (2)$$

$\omega = \frac{2\pi}{T}$ is the angular velocity of the wave,
T is the period of the wave, and a function of L and d.

The foregoing theory which gives a satisfactory description of the flow in the main body of the water neglects the effect of friction created by the presence of the solid boundary at the bottom. In the case of a real fluid, such as water, there is no slip of the fluid particles in contact with the bed. Within a thin layer adjacent to the boundary the flow is governed by the internal friction of the fluid and possesses the characteristics of a shear flow.

Depending upon the intensity of the wave action, this shear flow can be either laminar or turbulent. This problem has been investigated at the Hydraulics Laboratory of the University of California by Li and Manohar.[7][9] For practical reasons the experimental work was performed in a flume under reversed flow conditions in which the main body of the water was kept still and the bottom was oscillated according to a simple harmonic motion of the form.

$$u = a'_b \omega \sin \omega t$$

The water particles in contact with the wall oscillate with the same motion as the wall. This motion is transmitted by internal friction to the adjacent layers of fluid which are set into an oscillatory motion approximating closely a simple harmonic motion. The water particles oscillate with the same period as the wall but with amplitudes and phases varying with the distance from the bottom. As will be shown later, the amplitude of the velocity decreases very rapidly with the distance from the boundary so that one can consider that motion practically exists only within a thin layer adjacent to the boundary and called a boundary layer. It is assumed that no motion of any significance occurs beyond the limit of this layer. In the prototype as is shown on Figure 1, the conditions are similar but reversed. In the main body of the water, the flow is potential while near the solid boundary and within the boundary layer shear flow occurs. Water particles

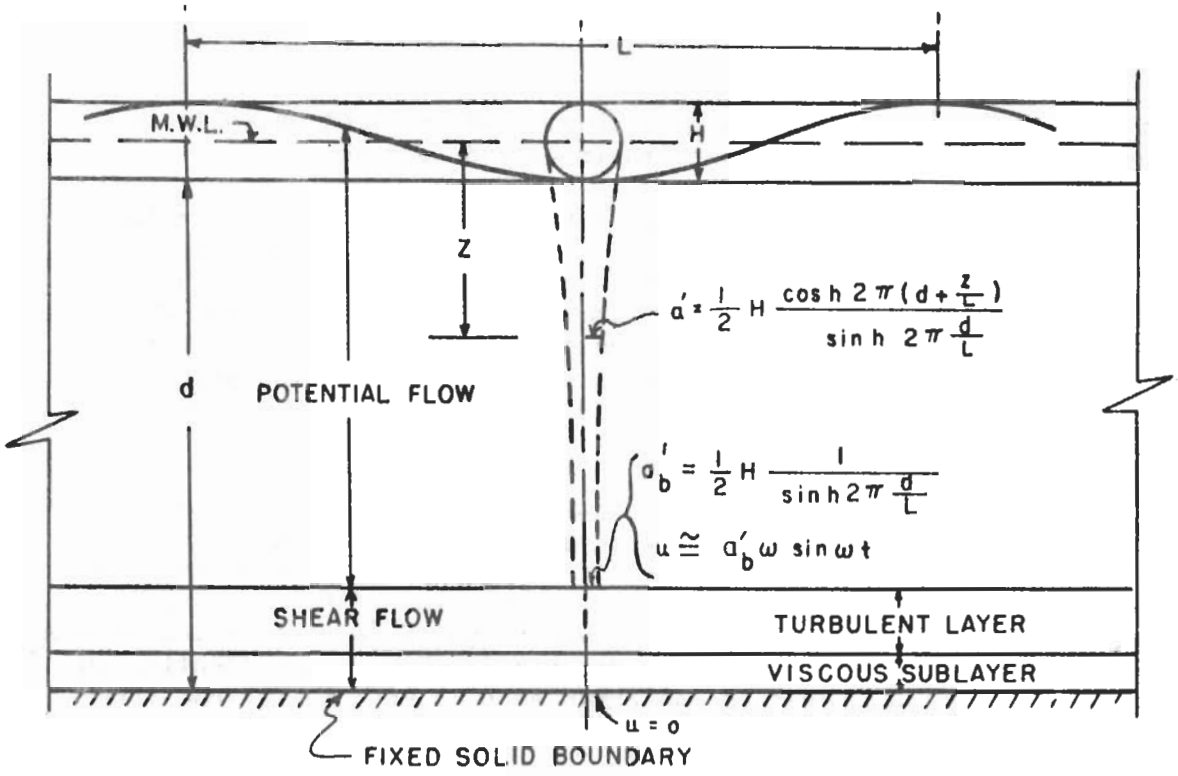

(a) PROTOTYPE FLOW CONDITIONS

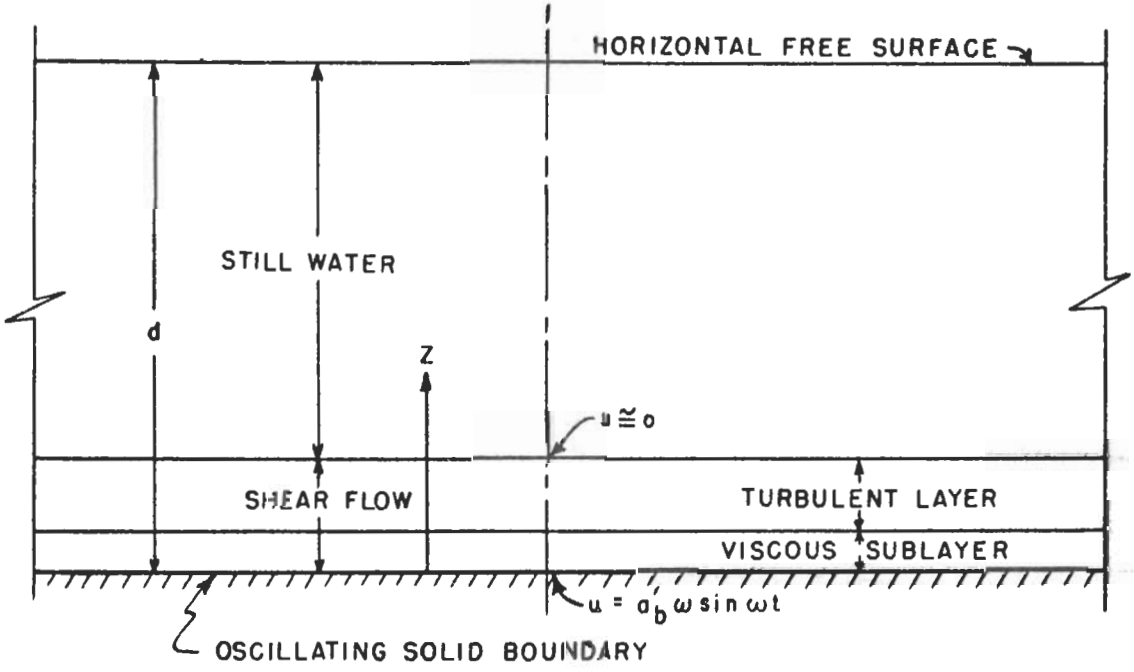

(b) MODEL FLOW CONDITIONS

FIG. 1 SKETCHES OF FLOW CONDITIONS

at the interface oscillate with a simple harmonic motion while in contact with the solid boundary their motion is zero.

It is evident under such circumstances that a certain similarity exists between the flow patterns in the boundary layers of the two cases. Since for practical reasons it is very difficult to duplicate actual prototype conditions, the results obtained by studying the model are very valuable in providing certain information regarding the behavior of the flow in the actual case. The present study investigates model conditions only and deals with the hydraulics near an oscillating smooth wall.

Li experimented with a hydraulically smooth oscillating wall as well as with rough walls of two dimensional roughness varying in type and size. He studied the effect of the amplitude, the period and the kinematic viscosity of the water on the type of flow and he determined a Reynold's number which was found to be a criterion between laminar and turbulent condition. Manohar[7] later, experimenting on the same flume, has verified and extended Li's work to include three dimensional roughness.

By using Li's and Manohar's criteria it is possible to predict whether the flow in the boundary layer will be laminar or turbulent for any set of values of amplitude, period, kinematic viscosity of water, and type and size of roughness. The present study attempts to solve the problem of predicting the velocity distribution in the boundary layer for the turbulent case and for a smooth wall. The problem of the laminar case has already been solved long ago, but a brief presentation of its main points is deemed helpful as an introduction to the subject of the turbulent case.

LAMINAR CASE

Let us consider the case of a hydraulically smooth wall of infinite extent in the xy plane which oscillates with a simple harmonic motion in the x direction. The fluid is assumed to fill the half space $z \geq 0$. It is further assumed that flow in the entire half-space is characterized by oscillating velocities in the x direction only, which are of the same period as that of the wall. The flow velocity is thus a function of z and t only. If the fluid is assumed to be homogeneous the equation of motion can in that case be written as

$$\frac{\partial u}{\partial t} = \nu \frac{\partial^2 u}{\partial z^2} \qquad (3)$$

where the kinematic viscosity ν, is a constant for the entire half space. Lamb[6] gives a solution of equation (3) which may assume the form

$$u = a'_b \omega e^{-\beta z} \sin(\omega t - \beta z) \qquad (4)$$

where $$\beta = \sqrt{\frac{\omega}{2\nu}} \qquad (5)$$

It may be noticed that this solution satisfies the boundary conditions

$$u = a'_b \omega \sin \omega t \qquad \text{for } z = 0$$

and $$u = 0 \qquad \text{for } z = a$$

Equation (4) represents a transverse wave propagated inward from the boundary with a wave length

$$\lambda = \frac{2\pi}{\beta} = 2\pi \sqrt{\frac{2\nu}{\omega}} \qquad (5a)$$

and with a velocity

$$c^o = \frac{\omega}{\beta} = \sqrt{2\nu\omega} \qquad (5b)$$

The amplitude reduces rapidly with the distance z from the bottom.

If one defines the limit of the boundary layer as the level where the amplitude of the motion is reduced to 1/100 of the amplitude at the bottom the thickness of this layer becomes

$$\delta_1 = \frac{4.6}{\beta} = 6.5\sqrt{\frac{\nu}{\omega}} \qquad (6)$$

Under ordinary wave conditions ν is about 10^{-5} ft^2/sec and ω = $1^{rad}/sec$.

Then $$\delta_1 = \frac{4.6}{\sqrt{10^{-5}}} = 0.0205 \text{ ft.} \qquad (6a)$$

$$\lambda = 0.028 \text{ ft.} \qquad (6b)$$

and $$c^o = 0.0045 \text{ ft./sec.} \qquad (6c)$$

TURBULENT CASE

When the flow becomes turbulent the fluid particles cease to follow parallel paths as in the case of laminar flow. The molecular exchange of momentum gives way to momentum or vorticity exchange of large masses of fluid which move temporarily as a unit and then mix with other masses. The problem of the unidirectional turbulent flow along a frictional boundary has been approached statistically by means of similarity methods(10). Not much progress has been made towards the investigation of an oscillatory turbulent flow. The objective of the present study is to derive a description of the turbulent flow of a real fluid near a smooth wall which oscillates with a simple harmonic motion in its own plane. The problem has been approached simultaneously from both the theoretical and the experimental point of view.

Theoretical consideration

As has been shown previously, the distribution of velocities along a normal section for the laminar case is given by a solution of the

equation of motion (equation (3))

$$\frac{\partial u}{\partial t} = \nu \frac{\partial^2 u}{\partial z^2} \qquad (3)$$

which satisfies the boundary conditions

$$u = u_o \sin \omega t \qquad \text{for } z = 0$$

and

$$u = 0 \qquad \text{for } z = \infty$$

The kinematic viscosity ν is constant for the particular fluid and for constant temperature.

In dealing with the turbulent case, the determination of a differential equation of motion based on the concept of the equilibrium of the local instantaneous forces and hence the derivation of a solution satisfying the boundary conditions becomes very difficult. Recourse has been made to the already established relationships of the unidirectional flow. Boussinesq[2] in his classical theory of the description of turbulent flow was the first investigator to express the shear stress in a way similar to the one for the laminar case by introducing the coefficient ϵ . The shear stress is then given by the expression

$$\frac{\tau}{\rho} = -\epsilon \frac{\partial u}{\partial z} \qquad (7)$$

ϵ has the dimensions of kinematic viscosity ν and it is usually referred to in the literature as eddy or mechanical viscosity. Prandtl[10] later proposed a theory by which the coefficient ϵ was related to the mixing length ℓ', which in turn is defined as the distance normal to the direction of the main flow which a fluid particle must travel with the mean property of its origin, before it mixes effectively with the surrounding fluid and thereby assumes the property of the flow in its new location. The mixing length ℓ' and the coefficient ϵ have generally different values for the exchange of different properties. So depending upon the case considered, use is made of the expressions mixing length and/or coefficient, of momentum exchange, of heat exchange, of vorticity exchange (etc.).

A simple form of the equation of motion for a two dimensional incompressible turbulent flow is the following[4]

$$\frac{\partial u}{\partial t} = \epsilon_v \frac{\partial^2 u}{\partial z^2} \qquad (10)$$

where ϵ_v is the coefficient of vorticity exchange and a function of z only.

In the case of unidirectional turbulent flow, it is assumed that the motion at any horizontal plane can be separated into a mean flow and superposed turbulent fluctuations, the mean value of which is zero. In the present case, the mean flow is variable. It is then necessary

to assume that the fluctuations are so rapid that a significant mean velocity can be taken in an interval which is short enough that the change in the mean flow during that interval can be neglected[4]. Thus we are dealing here with mean velocities, but for reasons of simplification, the bars are omitted.

Again as in the laminar case, the main flow velocity is assumed to have a component in the x direction only, which at all distances z is a simple harmonic motion with the same period as that of the wall. The effect of turbulence is presumably described by ϵ_v .

In order to correlate the experimental results with the theory the velocity component in the x direction was assumed to take the form

$$u_{(z,t)} = A \sin(\omega t - B) \tag{11}$$

The parameters A and B were left open.

Equation (11) is a satisfactory solution for our problem if functions A and B can be found that satisfy the differential equation (10) including boundary conditions and also describe the experimental measurements. Equation (11) may be written in the form of a complex expression

$$u_{(z,t)} = A\, e^{i(\omega t - B)} \tag{11a}$$

which in turn can be a solution of an equation similar to equation (10).

It is assumed here that A and B are functions of z only. Thus

$$\frac{\partial u}{\partial t} = i A \omega e^{i(\omega t - B)} \tag{12}$$

$$\frac{\partial u}{\partial z} = \left[A_z - iAB_z\right] e^{i(\omega t - B)} \tag{13}$$

$$\frac{\partial^2 u}{\partial z^2} = \left[A_{zz} - 2iA_z B_z - iAB_{zz} - AB_z^2\right] e^{i(\omega t - B)} \tag{14}$$

By substituting in equation (10) and after dividing all terms by $e^{i(\omega t - B)}$ we obtain

$$iA\omega = \epsilon_v \left[A_{zz} - 2iA_z B_z - iAB_{zz} - AB_z^2\right] \tag{15}$$

By separating real and imaginary parts, we obtain two simultaneous differential equations:

$$A_{zz} - AB_z^2 = 0 \tag{16}$$

and

$$A\omega = -\epsilon_v \left[2A_z B_z + AB_{zz}\right] \tag{17}$$

If one of the three functions A, B and ϵ_v is known, the other two can be deduced from equations (16) and (17). From the experiments, as will be shown later, it was possible to determine the function A. It can be given as a power function of z of the form

$$A = K z^c \tag{18}$$

where K is a constant and c is a negative exponent then

$$A_z = K c z^{c-1} \tag{19}$$

$$A_{zz} = K c (c - 1) z^{c-2} \tag{20}$$

By substituting in equation (16) we obtain

$$B = \sqrt{c (c - 1)} \log_e K_2 \frac{z}{z_o} \tag{21}$$

K_2 is a constant and z_o is an arbitrary length scale.

From equation (21) we obtain

$$B_z = \frac{\sqrt{c (c-1)}}{z} \tag{22}$$

and

$$B_{zz} = -\frac{\sqrt{c (c-1)}}{z^2} \tag{23}$$

After substituting in equation (17) we deduce

$$\epsilon_v = \frac{\omega z^2}{(1 - 2c) \sqrt{c(c - 1)}} \tag{24}$$

The arbitrary length scale z_o can be determined by assuming that z_o is the distance from the wall at which the coefficient ϵ_v is equal to ν. Thus

$$\epsilon_v(z_o) = \frac{\omega z_o^2}{(1 - 2c)\sqrt{c(c - 1)}} = \nu \tag{25}$$

and

$$z_o = \sqrt{\frac{\nu}{\omega}} \left[(1 - 2c)\sqrt{c(c-1)}\right]^{\frac{1}{2}} \tag{26}$$

Equation (11) finally becomes

$$u_{(z,t)} = K z^c e^{i(\omega t - a \log_e K_2 \frac{z}{z_o})} \tag{27}$$

or

$$\frac{u}{u_o} = K_3 z^c e^{i(\omega t - a \log_e K_2 \frac{z}{z_o})} \tag{28}$$

Where $u_o = a^* b \omega$ = the maximum velocity of the oscillating wall and

$$a = \sqrt{c\,(c-1)} \qquad (28a)$$

If we put $K_3 = \frac{K_4}{z_o^c}$ equation (28) becomes

$$\frac{u}{u_o} = K_4 \left(\frac{z}{z_o}\right)^c e^{i(\omega t - a \log_e K_2 \frac{z}{z_o})} \qquad (29)$$

or in its real form:

$$\frac{u}{u_o} = K_4 \left(\frac{z}{z_o}\right)^c \sin\left(\omega t - \sqrt{c(c-1)} \log_e K_2 \frac{z}{z_o}\right) \qquad (29a)$$

This solution of the equation of motion (equation 10) can be used in describing the flow within the observed range of distance from the bottom in the case of turbulent oscillatory flow. The constants K_2 and K_4 and the exponent c, are to be determined experimentally.

Equation (29a) indicates that the amplitude of the velocity is a power function of z as has been assumed. The phase shift turns out to be a logarithmic function of z in contrast to the linear phase shift of the laminar law (equation 4).

However, this solution has two drawbacks; first it loses significance for values of z close to zero for which the amplitude approaches infinity. In other words, it fails to give a reasonable description of the flow at small distances from the wall. This may not be very serious if one remembers that the logarithmic flow formula in unidirectional flow,[10] also breaks down near the solid boundary. It may be assumed that in the case of an oscillatory flow a viscous sublayer must also be introduced between the turbulent flow and the boundary, in order to describe actual flow conditions. The reference level z_o is arbitrarily taken as the distance from the solid boundary at which the coefficient of vorticity exchange, ϵ_v, is equal to the kinematic viscosity. This distance is believed to be of the same order of magnitude as the thickness of the viscous sublayer. No attempt is made in this study to measure or to predict flow conditions in this sublayer.

Second, it is not possible to determine the shear stress which is given by the expression[4]

$$\frac{\tau}{\rho} = -\epsilon_m \frac{\partial u}{\partial z} \qquad (30)$$

from the solution of equation (10), because ϵ_m in equation (30) is the coefficient of momentum exchange, a parameter quite different from ϵ_v, the coefficient of vorticity exchange which is given by equation (24).

In addition to the model described by equation (10), the following equation of motion which describes the turbulent momentum exchange was

investigated:

$$\frac{\partial u}{\partial t} = \frac{\partial}{\partial z}\left(\epsilon_m \frac{\partial u}{\partial z}\right) \tag{31}$$

where ϵ_m is the coefficient of momentum exchange.

It is assumed again that the velocity u of the main flow is given by an expression similar to equation (11a)

$$u_{(z,t)} = A_1 e^{i(\omega t - B_1)} \tag{32}$$

Where A_1 is again a power function of z and B_1 a logarithmic function of z of the form

$$B_1 = K_1 \log z \tag{33}$$

Omitting the repetition of the calculations which are similar to the one for equation (10), the following results were obtained:

$$a_1 = \sqrt{c\,(c+1)} \tag{34}$$

$$\epsilon_m = -\frac{\omega z^2}{(2c+1)\sqrt{c\,(c+1)}} \tag{35}$$

and

$$B_1 = \sqrt{c(c+1)}\,\log_e z \tag{36}$$

Consequently equation (32) becomes

$$\frac{u}{u_o} = K_4'\left(\frac{z}{z_o}\right)^c e^{i\left(\omega t - \sqrt{c(c+1)}\,\log_e K_2' \frac{z}{z_o}\right)} \tag{37}$$

and in its real form

$$\frac{u}{u_o} = K_4'\left(\frac{z}{z_o}\right)^c \sin\left(\omega t - \sqrt{c(c+1)}\,\log_e K_2' \frac{z}{z_o}\right) \tag{37a}$$

Where K_2', K_4' are constants and z_o an arbitrary length scale, equations (35) and (36) indicate that the coefficient of momentum exchange ϵ_m and the phase shift function B_1, have significance only when $c < -1$.

The measurements showed that $c = -0.65$ which indicates that either equation (37a) is not the right form of solution of equation (31) or equation (31) is not applicable in describing this type of motion.

Experimental work

Chronologically the experimental work preceded the theory. The mathematical approach was oonsidered only after the experimental data

had already been obtained and was in the process of being analyzed.

The fundamental idea though was the same. The basic concept was that the distribution of the velocity along the vertical could be expressed in a similar way to the laminar case.

If nothing were known about the theoretical solution, the description of the flow could be given by equation (38)

$$\frac{u}{u_o} = f_1(z) \sin\left[\omega t - f_2(z)\right] \qquad (38)$$

where u_o is the amplitude of the velocity at the bottom.

Assuming that the theoretical solution given by equation (29) is correct, the functions of equation (38) must be

$$f_1(z) = K_4 \left(\frac{z}{z_o}\right)^c$$

$$f_2(z) = \sqrt{c(c-1)}\, \log_e K_2 \frac{z}{z_o}$$

This can easily be verified from measurements.

a. Apparatus

The same apparatus used previously by Li and Manohar was also used in this work. A picture of it is shown on figure (2) and a schematic diagram on figure (2a). The main features are a glass wall flume 12 feet long by one foot wide and 3 feet deep. A stainless steel platform 11½ inches wide by 6½ feet long oscillates on two sets of rollers supported by two rails which are bolted to the bottom of the flume. A ½-horsepower AC motor provides the moving power. Through an eccentric arm and linkage the rotating motion of the motor is converted into a reciprocal motion which closely approximates a simple harmonic motion. Through a stainless steel band 3/4 of an inch wide, this motion is transmitted to the platform. The band was later replaced by a steel piano wire which, because of its smaller mass, transmitted less vibrations to the platform. The period of the motion is regulated by a speed reducer which covers a range of frequencies between 1 and 150 cpm. The amplitude of the linear motion of the platform is controlled by the adjustable length of the eccentric driving arm. The range of the semi-amplitudes is from 2½ inches to 4 feet. The water was usually kept at a depth of 2 feet. The flume is relatively short compared to the displacements of the platform. This gives rise to the creation of standing waves.

The character of these waves is rather complex, but their main component is a sinusoidal wave of the same period as the motion of the platform but of different phase and of varying amplitude. In order to

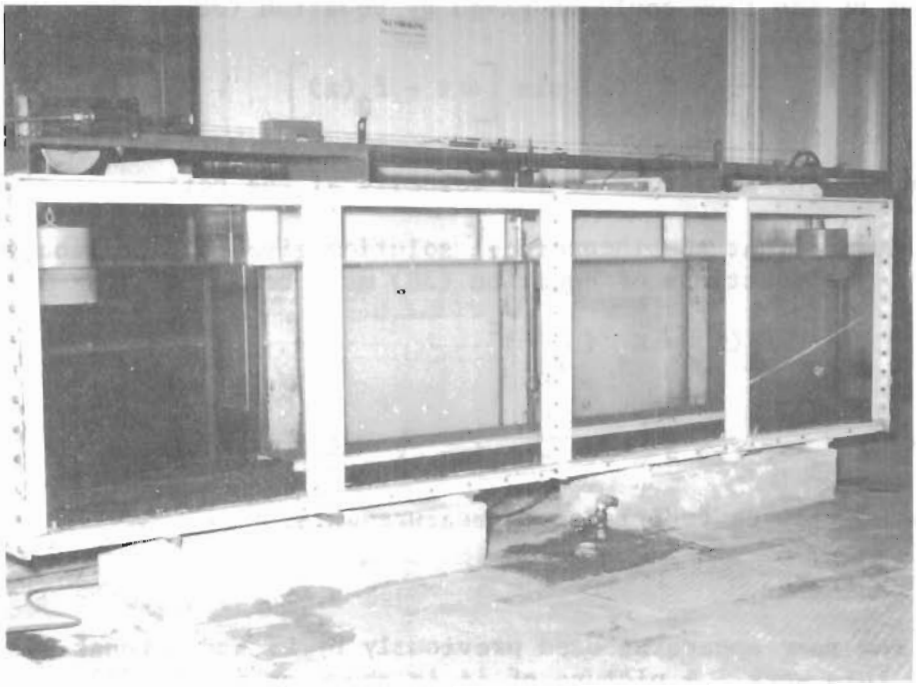

FIG. 2 TEST FLUME

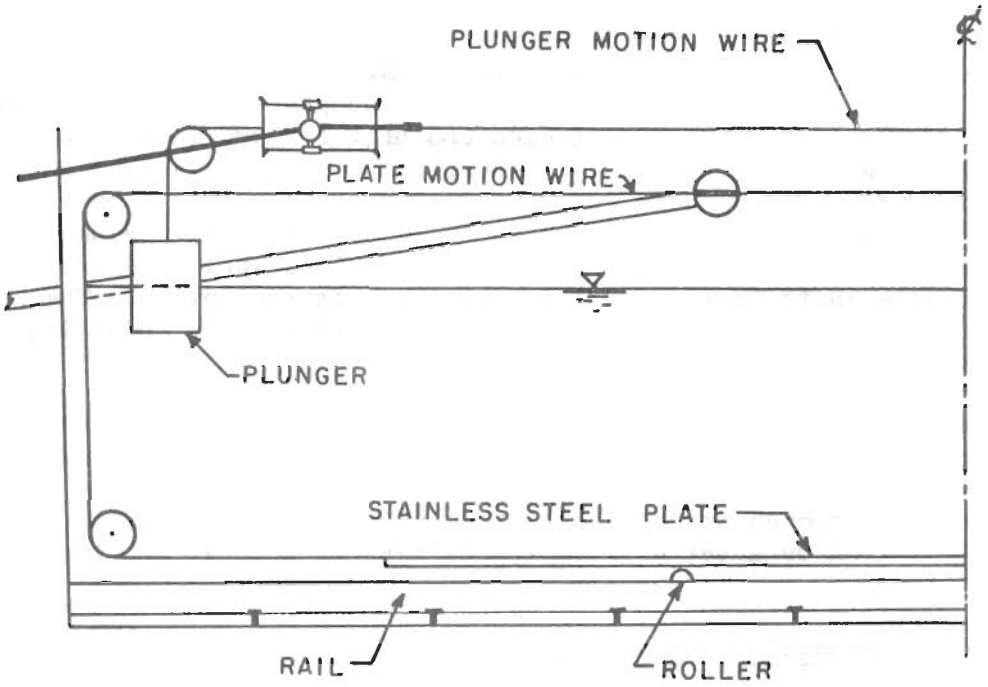

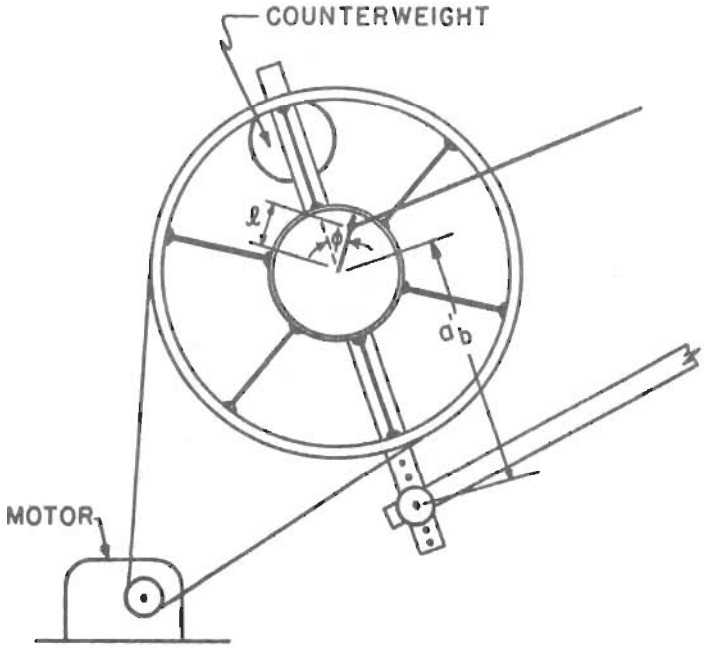

a'_b = ADJUSTABLE AMPLITUDE OF PLATFORM MOTION

ℓ = ADJUSTABLE AMPLITUDE OF PLUNGER MOTION

ϕ = ADJUSTABLE PHASE SHIFT OF PLUNGER MOTION

FIG. 2 a SCHEMATIC DIAGRAMS OF THE FLUME AND OF THE DRIVING MECHANISM USED IN THE EXPERIMENT

eliminate the effect of this standing wave, an arrangement has been devised, a schematic diagram of which is shown on figure (2a). The system mainly consists of two cylindrical plungers 8 inches in diameter and 10 inches high suspended at each end of the flume in such a way as to be about half-submerged. Through an arm and a crank, the wire connecting the two plungers gets a rectilinear oscillating motion from the driving mechanism. The phase shift is effected by turning the disc on which the arm is connected at any desired angle $\Delta \phi$ with respect to the shaft from which the platform gets the motion. The amplitude ℓ of the plunger motion can be controlled by adjusting an eccentric.

For a given condition of motion of the platform, the proper combination of phase shift and amplitude was always found empirically as that which eliminated to the greatest extent the standing wave effect. The remaining components of higher frequencies and small amplitudes were eliminated by a set of floating baffles located at the two ends of the flume.

b. Experimental methods and procedures

1. Photographic method for measuring instantaneous velocities.

A first method used in the attempt to determine the functions $f_1(z)$ and $f_2(z)$ of equation (3.8) was based on the idea of measuring the horizontal displacement of water particles at given distances from the bottom within known time intervals. Values of the local velocities are obtained by dividing the displacements by the corresponding time intervals. The horizontal distances traveled by the water particles were determined optically. White colored particles of liquid visible to the naked eye were inserted into the flow from the top of the flume through a thin glass dropper. A mixture of mineral oil and carbon tetrachloride with white zinc paste in proportions to give a density equal to that of water was used. The paths traveled by the white colored particles were recorded by taking multiple exposure pictures at eaual time intervals. Two photographic cameras were alternately used for taking pictures; a 35-mm "Exacta" and a 4-inch by 5-inch "Graflex". Each time the camera was set at a distance of about 3 feet from the flume and at a level of about 2 inches above the platform. The number of pictures taken on the same frame was equal to the number of flashes of a strobovolume lamp. A strobotag apparatus adjusted to flash usually twenty-four times per period of oscillation regulated the flashing frequency of the strobovolume lamp.

Governed by a contact switch attached to the main drive shaft, the lamp was only operating during half the period of the oscillation, the first flash coinciding with the beginning of the stroke. After a large number of pictures was taken for half the period of various flow conditions, the procedure was repeated for the other half. This way a record of the history of the flow at various levels was obtained. A screen divided in squares of one-tenth of a foot was placed in front

of the flume as a length scale. Afterwards a correction for distortion was made. The distances traveled by the particles during each time interval were then measured and the instantaneous velocities at each level and phase were computed. A typical picture taken this way is shown on Figure (3). Velocity distributions along the vertical for various fractions of the period could then be drawn. Unfortunately the results were not very satisfactory, for the following reasons:

a. It was difficult to constantly maintain the density of the particles equal to that of the water. The thickness of the layer where measurements were made was so small that the particles were occasionally hitting the bottom or thrown upwards away from the flow.

b. The method presumes a two dimensional flow. Actually, the motion has a component normal to the plane of the picture. The central projection neglects the effect of the third dimension and introduces an error which increases with increasing horizontal angle of projection. This error can be eliminated by using a second camera taking pictures on a horizontal plane.

c. Secondary motions in the form of circulations superimposed their effects on the main flow. The origination and nature of these motions were of very complicated character and therefore hard to control. In certain cases, their effect on the main flow was larger than the quantity under measurement. The flow records obtained from the pictures represent instantaneous displacements and velocities. This excludes the possibility of separating and eliminating systematic errors Trying to make accurate measurements under such conditions was very difficult if not impossible, and the method was finally abandoned.

2. Dye method for measuring the phase shift.

After the first method failed to give satisfactory results, another method was developed which helped to determine the function $f_2(z)$, or in other words, the law which governs the phase shift of the flow at different levels. An inspection of the expression for the laminar case (equation 4) reveals that the phase shift of the flow at a level with respect to the oscillation of the platform is a linear function of the distance z. When the dimensionless value ωt is plotted against the corresponding dimensionless value $z\sqrt{\frac{\omega}{\nu}}$ on log-log graph paper the relationship follows a straight line of slope 1 which passes through the point

$$z\sqrt{\frac{\omega}{\nu}} = \sqrt{2} \quad \text{for} \quad \omega t = 1 \qquad \text{(figure 5)}$$

The following method was used to investigate the same problem in the turbulent case.

A very thin filament of dye (potassium permanganate) was introduced into the flow, through a thin glass tube maintained rigidly

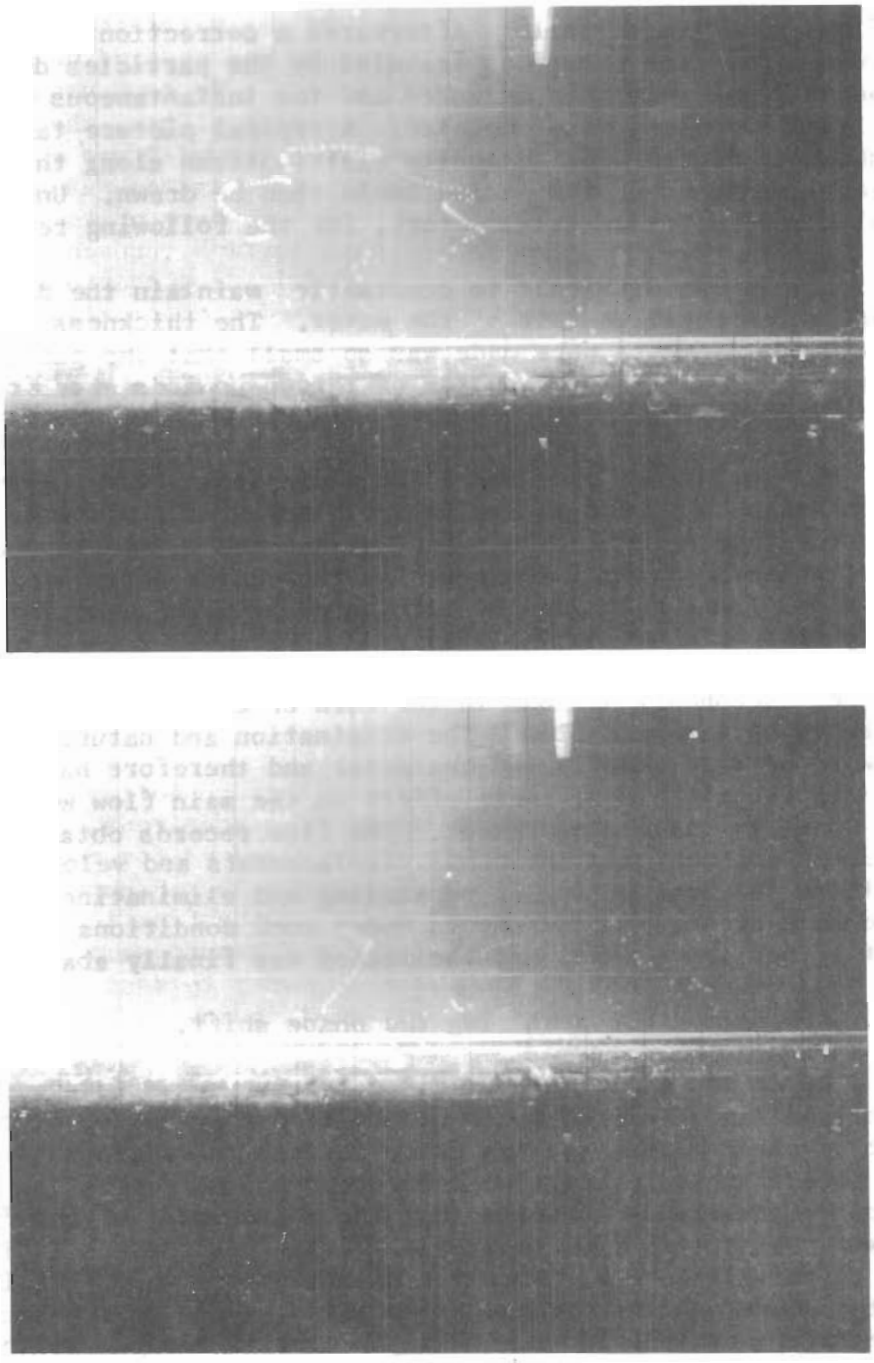

FIG.3 PHOTOGRAPHIC RECORDS OF THE MOTION OF FLUID PARTICLES

vertical in the flume. The flow of the dye was maintained constant with the use of a syphon. The entire system was mounted on a point gage with a least count of 0.001 foot. Figure (4). To compensate for eventual irregularities of the surface of the platform, the point gage was lowered to let the tip of the tube touch the platform at a number of positions. The average zero distance thus obtained was used as a basis of measurement. The time history of the phase of the platform was recorded by one needle of a Brush oscillograph through a contact switch activated by the main shaft of the driving mechanism. The other needle of the oscillograph was connected electrically to an ordinary push buttom. This button was operated manually by the observer each time the flow of the dye filament was changing direction. This way the time history of the phase of the flow at various levels was obtained. At each level the observation continued for a number of periods and then the individual recorded phase shifts were averaged out. A sketch of a typical record is shown in Figure (4). The plot of such data on log-log graph paper in a dimensionless form as before, yielded a straight line, but of a slope steeper than that of the theoretical laminar case (Figure 5). This indicates that within the range of measurements the phase shift law in the turbulent case is not a linear function of the distance from the bottom. No measurements were possible at distances less than 0.006 foot and more than 0.025 foot.

Most of the measurements were made on a rough bottom where the roughness elements consisted of semicircular wooden rods, 3/4 inch in diameter, glued to the platform. The data obtained for rough and smooth bottoms are shown on Tables I and II (Appendix A). Figure (5) shows the relationship between phase shift and distance from the bottom. The theoretical laminar curve is also shown for the purpose of comparison. Rough bottom conditions were used first in order to test the reliability of the method. Li[7] showed previously that in the case of a rough wall, turbulent flow occurs for smaller values of stroke than for a smooth wall at equal periods. The advantage of the rough bottom was that the major part of the undesirable secondary motions which occur at high values of either ω or a_b was eliminated.

The results obtained by this method were consistent, but not sufficient for the complete description of the flow, because no information was supplied regarding the decay of the motion for increasing distances from the bottom. Another method had to be developed by which direct measurements of the local velocities could be made.

3. Method using velocity measuring instrument.

A. Description of the instrument.

For this purpose a symmetric instrument similar to a Pitot tube was developed which was combined with an electronic indicator for measuring pressure differences. The electronic equipment is the same as used by Li in 1954[8]. It consists of a Rutishauser pressure

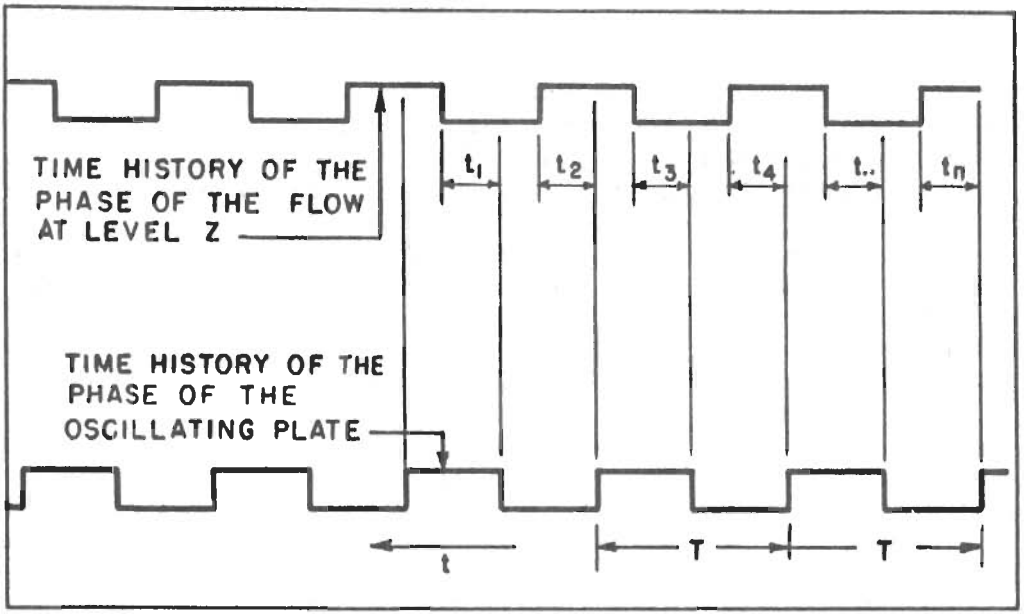

PHASE SHIFT $\Delta t = \frac{\Sigma t_i}{n}$

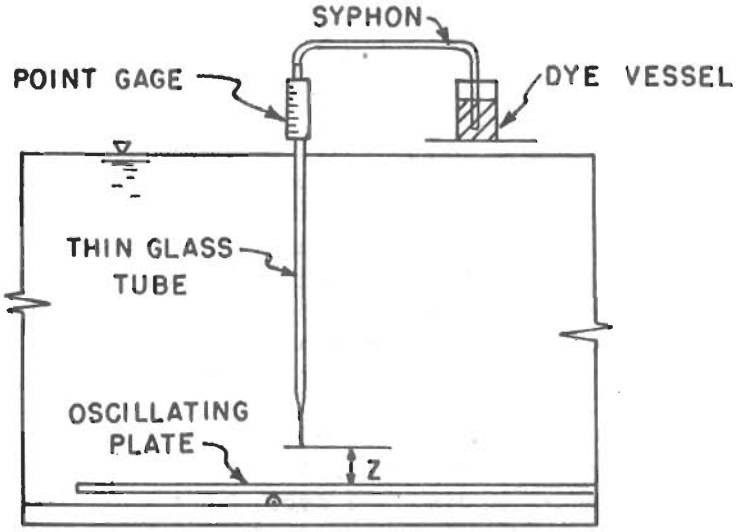

FIG. 4 SKETCHES OF A TYPICAL PHASE SHIFT MEASUREMENT RECORD AND OF THE APPARATUS USED FOR MEASURING THE PHASE SHIFT WITH THE DYE METHOD

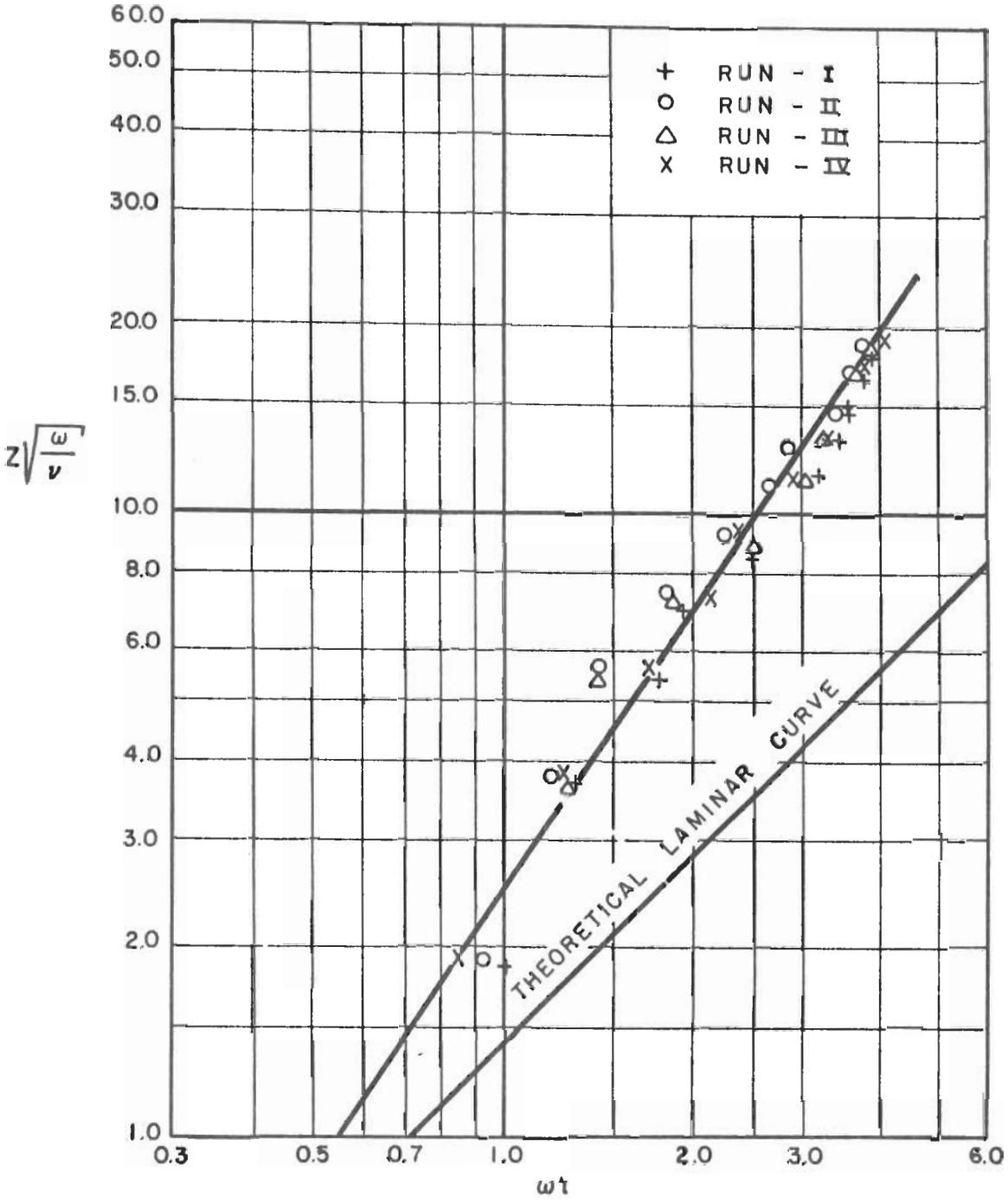

FIG. 5 PLOTTING OF EXPERIMENTAL DATA OF PHASE SHIFT MEASUREMENT WITH THE DYE METHOD.

ROUGH BOTTOM : $\frac{3}{4}$ IN. HALF ROUNDED WOODEN STRIPS

pickup, a modified Rutishauser pressure indicator (Type 910), a Tektronix Direct-Coupled Amplifier Type 112, and a Brush Universal analyzer with oscillograph. A block diagram and a picture of the arrangement is shown in Figure (6). With an ordinary steel diaphragm 3/16 inch in diameter and 0.001 inch thick, pressures in the range 0-1 psi can be measured. In the present case it was intended to measure maximum velocities of 1.0 ft./sec. corresponding to a pressure of 1.5 lb./sq.ft. or 0.01 psi. In other words, the sensitivity of the instrument had to be increased about one hundred times. This could be done by increasing the diameter of the diaphragm. After the 3/16-inch diaphragm was removed, the head of the Rutishauser pick-up was screwed into the top of an instrument which was designed especially in such a way as to combine a Pitot tube and the capacitor of the Rutishauser head. A section of the instrument is shown on Figure (7) and its properties are given in the following section.

B. Properties of the instrument. (Li[8])

I) Sensitivity: The theory of the forced vibrations of a circular thin plate clamped at the edge gives that the potential energy is

$$V = \frac{8\pi E T_o^3}{9(1-\sigma^2)\left(\frac{D_2}{2}\right)^2} X_c^2 = K X_c^2 \qquad (39)$$

where E = Young's modulus

σ = Poisson's ratio

T_o = Thickness of the plate

D_2 = Effective diameter of the plate

X_c = Displacement at the center.

The potential energy can also be estimated as

$$V = P a_o X_c \qquad (40)$$

where P = the pressure acting upon the plate and $a_o = \pi \frac{D_2^2}{4}$ is the effective area of the plate.

Substituting V in equation (39) with its value from equation (40) and solving for X_c, we obtain

$$X_c = \frac{9P(1-\sigma^2) D_2^4}{128 E T_o^3} \qquad (41)$$

For the standard steel Rutishauser diaphragm and for $P = 1.0$ psi

$$X_c = 2.63 \times 10^{-3} \text{ inches.}$$

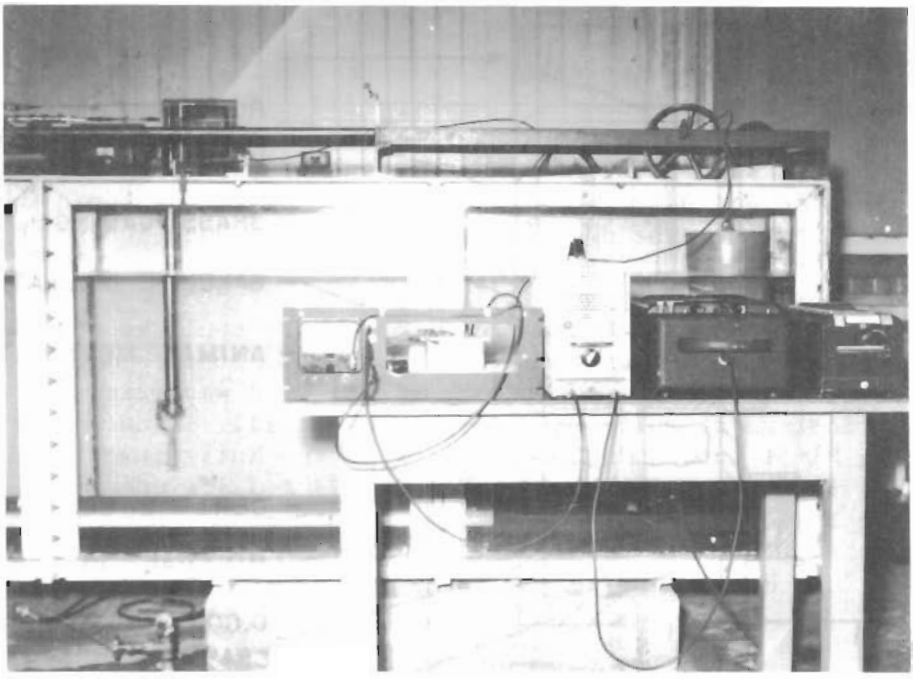

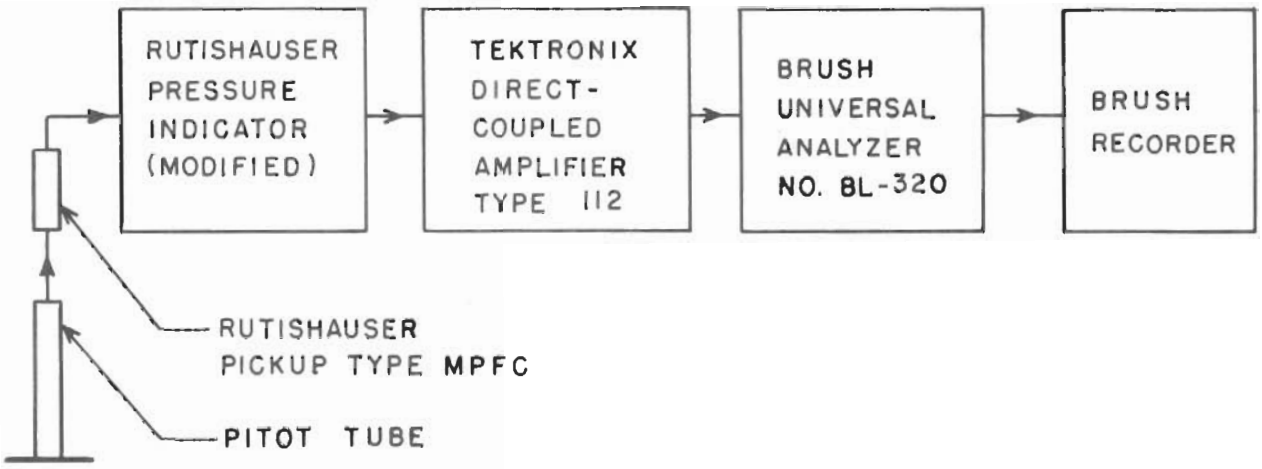

FIG.6 PHOTOGRAPH AND BLOCK DIAGRAM OF EXPERIMENTAL EQUIPMENT FOR VELOCITY MEASUREMENT

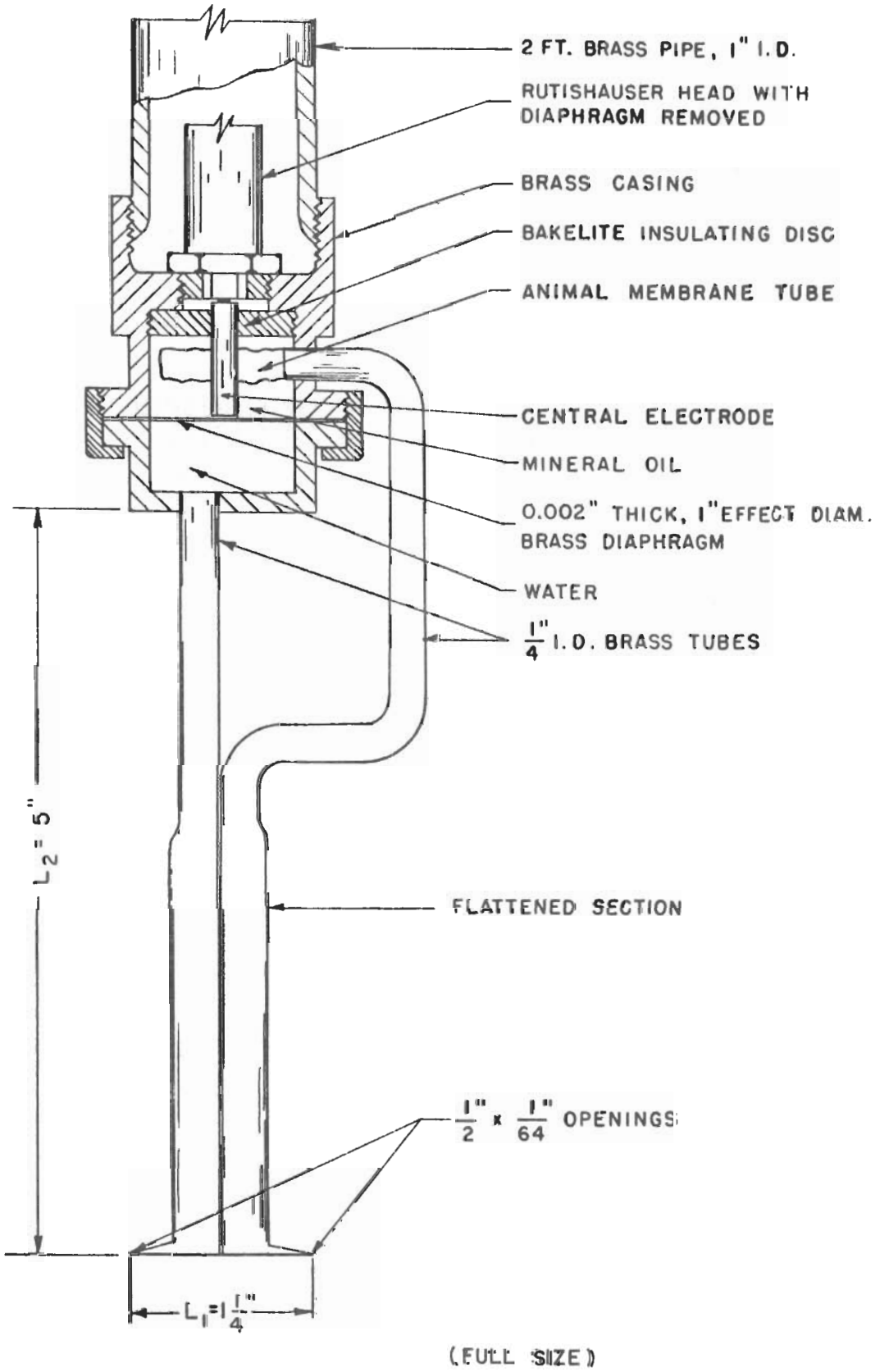

FIG. 7 SECTION OF VELOCITY MEASURING INSTRUMENT

For a brass diaphragm of $T_o = 0.002$ inch and for P = 0.01 psi, in order to have the same displacement the diameter should be $D_2 = 1.0$ inch.

II) Capacitance: The motion of the diaphragm in the Rutishauser gauge is recorded as the change of electric capacity between the diaphragm and a fixed electrode located close to it. This capacitance of the system is given by the expression

$$C_o = \frac{k\, A_o}{d_o} \tag{42}$$

where k is the dielectric constant of the fluid which fills the space between the electrodes; k for air has the value 1 and for oil about 2.

A_o is the area of the central electrode in square inches and d_o is the distance in inches between the central electrode and the diaphragm.

In order that the new instrument have the same capacitance as the standard Rutishauser head, the following condition must be satisfied:

$$\frac{k_a A'_o}{d'_o} = \frac{k_o A''_o}{d''_o} \tag{43}$$

where $d'_o = 0.0016$ inch, $\frac{k_o}{k_a} = 2$

and $A'_o = A''_o$

Consequently $d''_o = \frac{k_o}{k_a} d'_o = 2\, d_o = 0.0032$ inch.

In other words, the circular brass diaphragm should be placed at an average distance of 0.0032 inch from the central electrode.

III) Frequency response: As has been stated above, the potential energy of the diaphragm is

$$V = \frac{8\pi E T_o^3}{9 (1 - \sigma^2) \left(\frac{D_2}{2}\right)^2} X_c^2 .$$

Its kinetic energy is

$$T_1 = \pi \rho_m T_o \frac{\left(\frac{D_2}{2}\right)^2}{10} \left(\frac{dX_c}{dt}\right)^2 , \tag{44}$$

where ρ_m is the density of the diaphragm.

Thus the natural frequency would be

$$\frac{q}{2\pi} = \frac{1}{2\pi}\left[\frac{80}{9}\cdot\frac{T_o^2}{(\frac{D_2}{2})^4}\cdot\frac{E}{(1-\sigma^2)\rho_m}\right]^{\frac{1}{2}} \qquad (45)$$

For brass $E = 16 \times 10^6$ psi, $\sigma = 0.33$

and $\rho_m = \frac{0.29}{32.2 \times 12}$ lb. sec.^{2}/in.^{4}

$T_o = 0.002$ in. and $D_2 = 1.0$ in.

$$q = 180 \times 10^4 \frac{T_o}{D_2^2} = 3.6 \times 10^3 \text{ cps.}$$

and $\frac{q}{2\pi} = 575$ cps.

The kinetic energy of the fluid in the horizontal and the vertical tubes of the Pitot tube is

$$T_3 = \frac{\pi}{72}\rho_w D_2^2\left\{\ell_o(\frac{D_2}{D})^2 + \ell_1(\frac{D_2}{D_1})^2\right\}(\frac{dX_c}{dt})^2 \qquad (46)$$

where

$\ell_o = 1.0$ inch $\qquad \ell_1 = 5.0$ inches

$D = 0.2$ inch $\qquad D_1 = 0.25$ inch

$$\frac{T_3}{T_1} = B_2 = \frac{5\rho_w}{9\rho_m}\frac{1}{T_o}\left[\rho_o(\frac{D_2}{D})^2 + \ell_1(\frac{D_2}{D_1})^2\right] = 7.3\frac{D_2^2}{T_o}$$

or $\quad B_2 = 3.65 \times 10^3$

The natural frequency of the system thus modified to include the kinetic energy of the water is

$$\frac{q''}{2\pi} = \frac{q}{2\pi}\frac{1}{\sqrt{1+B_2}} = \frac{575}{61.3} = 9.4 \text{ cps.}$$

The maximum frequency of the oscillating platform is 1 cps and the ratio 1/9.4 = 0.106 is sufficiently small to guarantee the necessary frequency response of the instrument.

C. Principle of the operation of the instrument.

When the instrument is inserted into the flow in such a way that the two openings point into the two directions of motion, the velocity head is at any moment converted into a differential pressure on the diaphragm. This pressure is proportional to the square of the local velocity. The deformation of the diaphragm due to the application of this pressure changes the capacitance of the system which in turn modulates the

frequency of a 10 megacycle oscillator.

This FM signal is rectified by a discriminator into a voltage which is proportional to the differential pressure on the diaphragm. This voltage is amplified by a DC amplifier and activates one of the two needles of a "Brush" oscillograph. The lateral displacements of the needle are theoretically proportional to the different pressures acting upon the diaphragm, or to the second power of the local velocities. The time history of the velocity components in the x direction at any level can thus be obtained.

D. Calibration.

Before its use, the instrument was calibrated. This operation was performed in the same flume where the actual measurements were made. The instrument was rigidly fastened to the driving mechanism while the platform was uncoupled and remained still. The instrument performed a simple harmonic motion of the form $u = a'_b \omega \sin \omega t$.

The objective of the calibration was to define the relationship between the lateral displacement y of the needle and the respective horizontal components of the velocity. The velocity has a 90 degree phase shift with respect to the acceleration and it reaches its maximum value in the middle of the stroke where the acceleration becomes equal to zero. This is why in each case from the entire record of the velocity, its maximum value only was used for calibration because at this point the effect of the acceleration is negligible.

This maximum velocity is picked up by the diaphragm as differential pressure and through the electronic equipment it is recorded as a maximum displacement of the needle. Figure 9(a) shows a typical section of the calibration record.

The other needle of the oscillograph was electrically connected to a contact switch on the main drive shaft. The time history of the oscillating motion was thus recorded. From this record the average period and the average angular velocity for a set of measurements were easily calculated. After a number of data were obtained for different values of a'_b and ω the maximum displacements y were measured on the graph and after being averaged they were plotted in a log-log graph against the corresponding values of $a'_b \omega$ (maximum velocity). As shown on Figure (8), all these points fall very close to a straight line with slope about two. This means that the velocities are approximately proportional to the square root of the displacements or the square root of the pressures to which the displacements are proportional. By using the method of least squares the equation of the line was found to be

$$u = 0.140\, y^{0.54} \qquad (47)$$

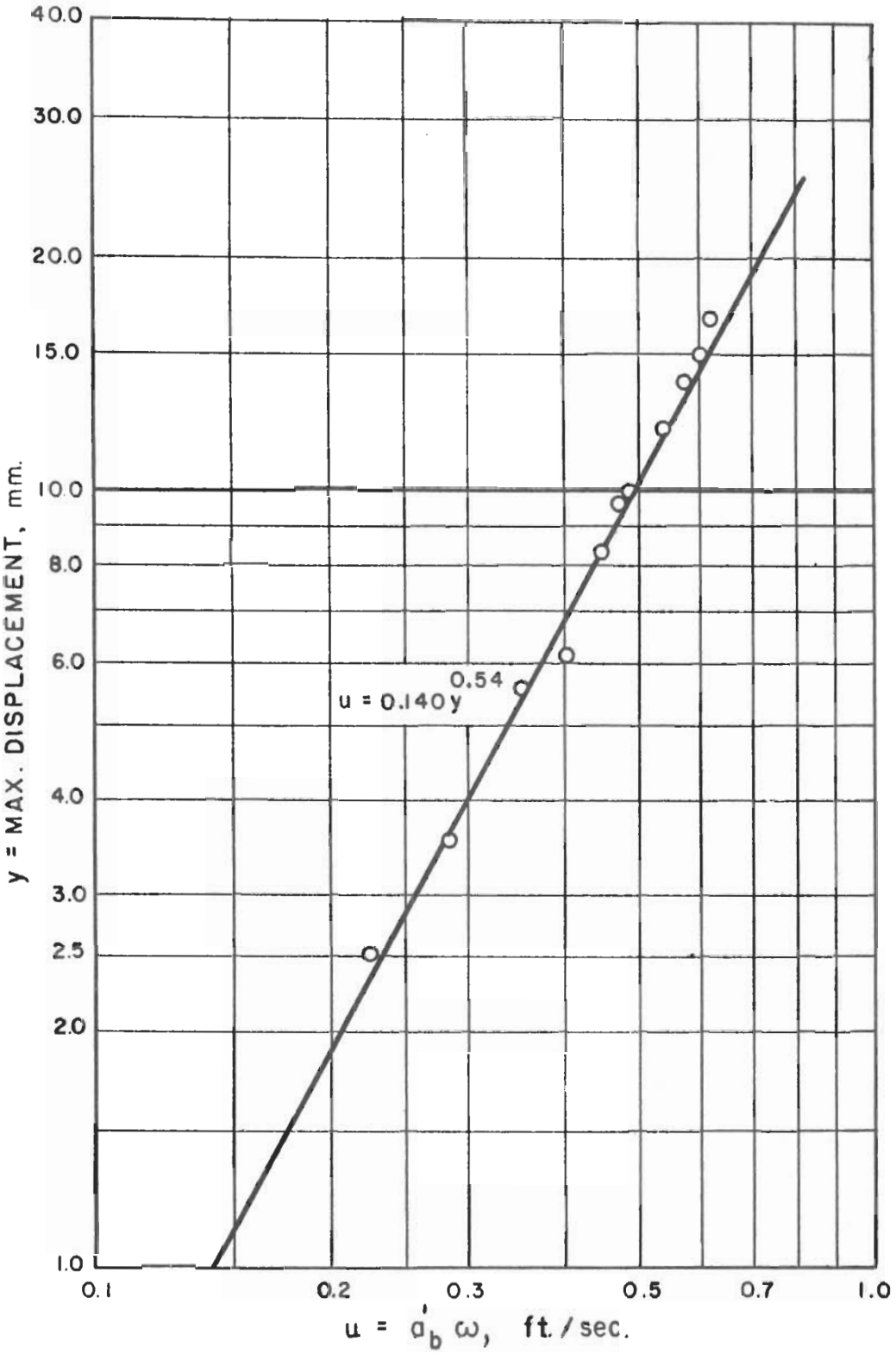

FIG. 8 CALIBRATION CURVE OF THE VELOCITY MEASURING INSTRUMENT

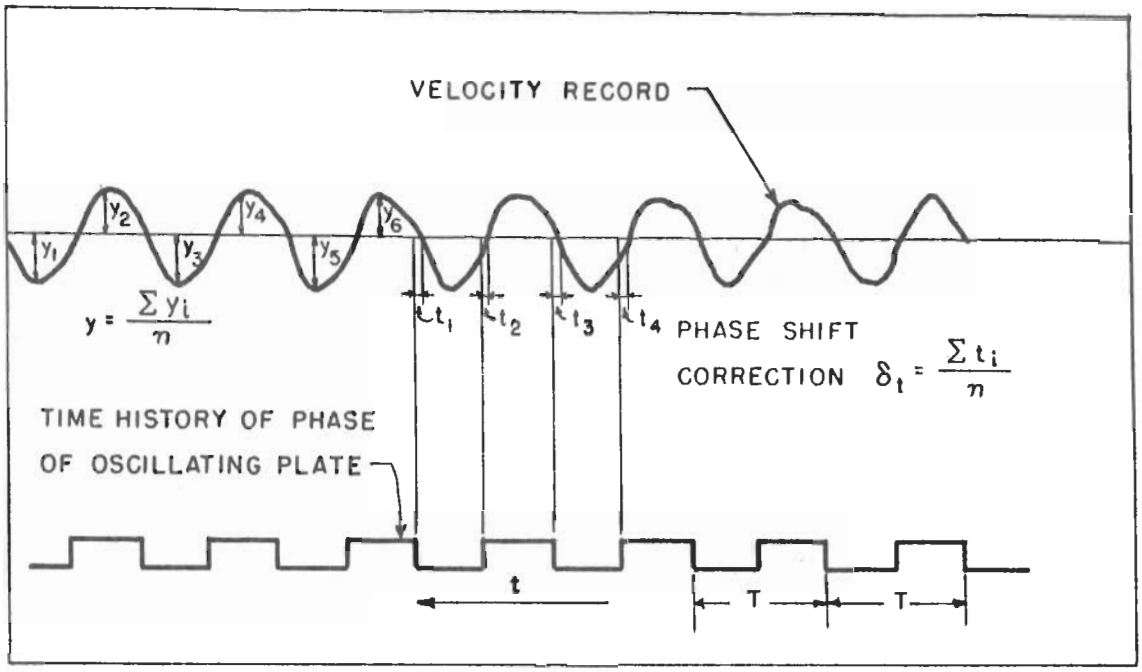

(a)

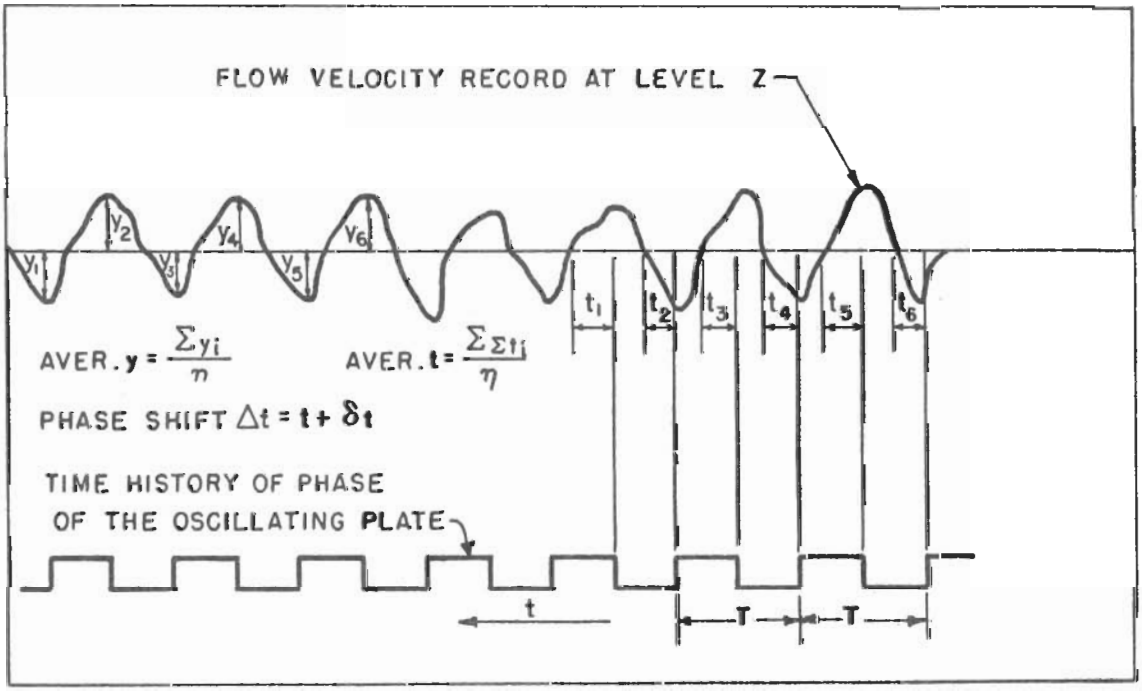

(b)

FIG. 9 SKETCHES - (a) OF TYPICAL CALIBRATION RECORD AND (b) OF TYPICAL VELOCITY MEASUREMENT RECORD

From this equation the amplitude of the velocity can be calculated from the corresponding maximum displacement y taken from the record.

c. Actual measurements and analysis.

The instrument was disconnected from the driving mechanism and was fastened at a vertical position in the flume. The distances of the openings from the bottom were measured with a point gage to an accuracy of 0.001 ft. The platform which was coupled again to the driving mechanism, oscillated with a simple harmonic motion. The layer of fluid near the moving platform was set into motion and after a number of oscillations, the equilibrium shear flow was established near the bottom. In all cases, the amplitude a'_b of the moving platform and its period $T = 2\pi/\omega$ were chosen such as to insure conditions of turbulent flow. Great care was taken to eliminate the effect of secondary motions. The same standing wave dampening device was used as before in the measurement of the phase shift. The record obtained was very similar to the one taken during the calibration (Figure 9(b)). The maximum displacements y for each set of values a'_b and ω and each distance z from the bottom were measured and averaged. This average value of y was inserted in equation (47) and a value for the average amplitude of the velocity was obtained. Table IV contains data taken by this method.

The ratio $\frac{u}{u_o}$, where $u_o = a'_b\omega$ was plotted on log-log graph paper against a Reynold's number of the form $N_R^{\frac{1}{2}} = Z\sqrt{\frac{\omega}{\nu}}$ Figure (10). The line connecting these points is essentially straight.

By applying the method of least squares, the equation of this line which determines the function $f_1(z)$ of equation (38) can be found.

Thus:

$$f_1(z) = 0.428\ (z\sqrt{\frac{\omega}{\nu}})^{-0.65} \tag{48}$$

For c = -0.65 the distance z_o of the reference level can be computed from equation (26).

Thus: $$z_o = 1.54\sqrt{\frac{\omega}{\nu}} \tag{49}$$

by substituting in equation (48) we obtain

$$f_1(z) = 0.360\ (\frac{z}{z_o})^{-0.65} \tag{48a}$$

and since it has been assumed that

$$f_1(z) = K_4\ (\frac{z}{z_o})^C$$

where C = -0.65, we deduce that:

$$K_4 = 0.360 \tag{50}$$

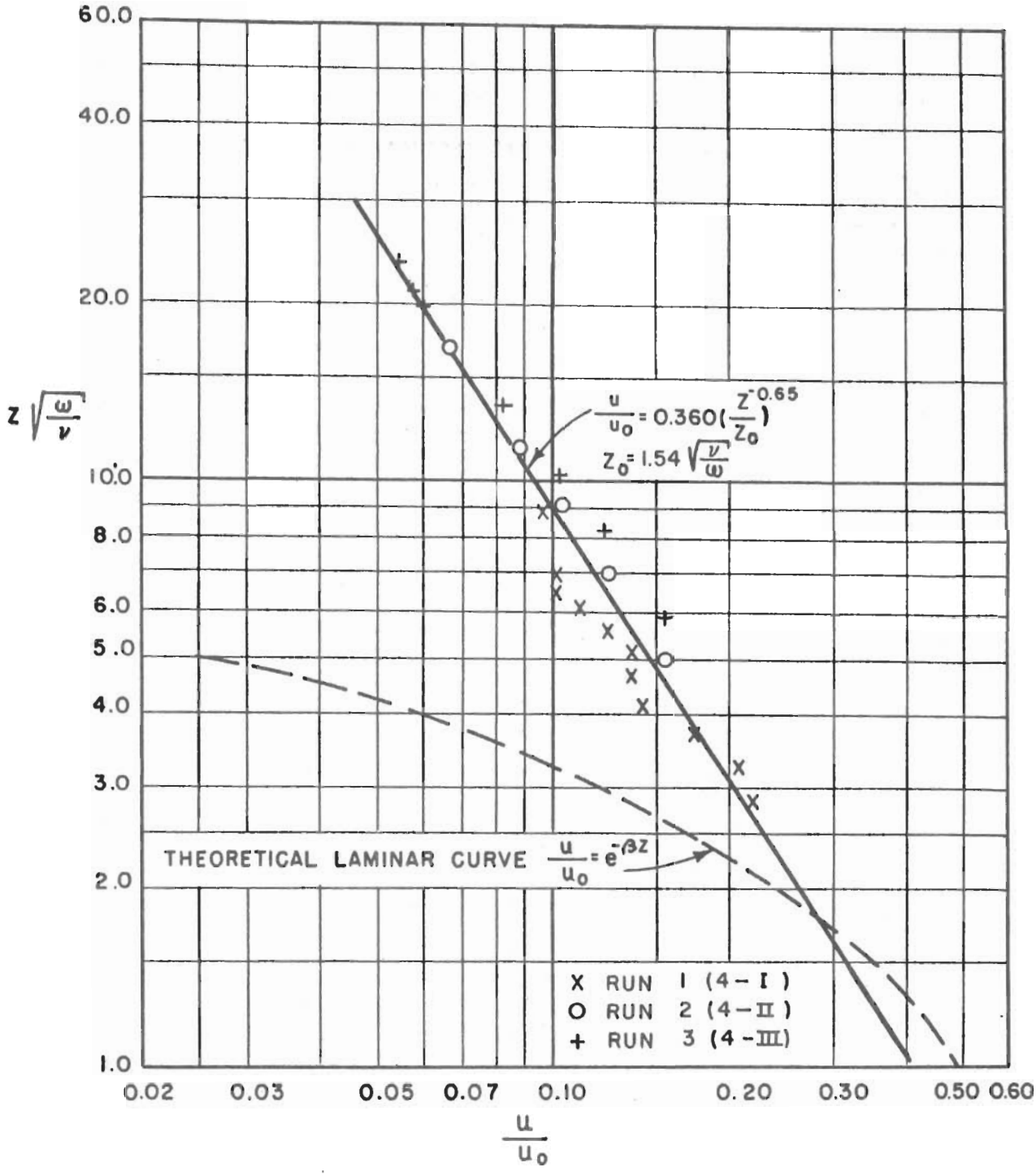

FIG. 10 PLOTTING OF EXPERIMENTAL DATA OF VELOCITY MEASUREMENT (SMOOTH BOTTOM)

In order to determine the second function of equation (38), the same method of dye used before has been used again. The data of measurements is listed on Table (V). The plotting of this data on a semi-log graph with the parameter ωt on the arithmetical scale and the Reynold's number $z\sqrt{\frac{\omega}{\nu}}$ on the logarithmic, shows the points falling closely on a straight line (Figure 11). The equation of this line found by the application of the method of least squares is

$$\omega t = 2.41 \log_{10} 2.04\, z\sqrt{\frac{\omega}{\nu}} \qquad (51)$$

but from equation (49) $\sqrt{\frac{\omega}{\nu}} = \frac{1.54}{z_o}$

After substitution equation (51) becomes

$$\omega t = 1.05 \log_e 3.14 \frac{z}{z_o} \qquad (52)$$

Thus the second function $f_2(z)$ is determined and found to be

$$f_2(z) = 1.05 \log_e 3.14 \frac{z}{z_o} \qquad (53)$$

The phase shift function of the theoretical solution, equation (29a), is found to be

$$B = \sqrt{c\,(c-1)} \log_e K_2 \frac{z}{z_o} \qquad (54)$$

When the experimental value of $c = -0.65$ is inserted in equation (54) we get

$$B = 1.04 \log_e K_2 \frac{z}{z_o} \qquad (55)$$

A comparison between equations (53) and (55) shows that the factor 1.04 which was deduced from the solution of the differential equation (10) checks very satisfactorily with the factor 1.05 obtained by experimental measurements. This is a very strong confirmation of the correctness of the theoretical solution. The constant K_2 was determined from equations (53) and (55) and found to be

$$K_2 = 3.14 \qquad (56)$$

Finally the two equations (29a) and (38) were combined into one expression of the form

$$\frac{u}{u_o} = 0.360 \left(\frac{z}{z_o}\right)^{-0.65} \sin\left(\omega t - 2.41 \log_{10} 3.14 \frac{z}{z_o}\right) \qquad (57)$$

where $z_o = 1.54\sqrt{\frac{\nu}{\omega}}$. Equation (57) is a solution of equation (10) and it also describes the experimental measurements. It is worth mentioning here that the phase shift function $f_2(z)$ was determined not only by the dye method described above, but from the velocity measurement records as well. The phase shift of the motion at the level where

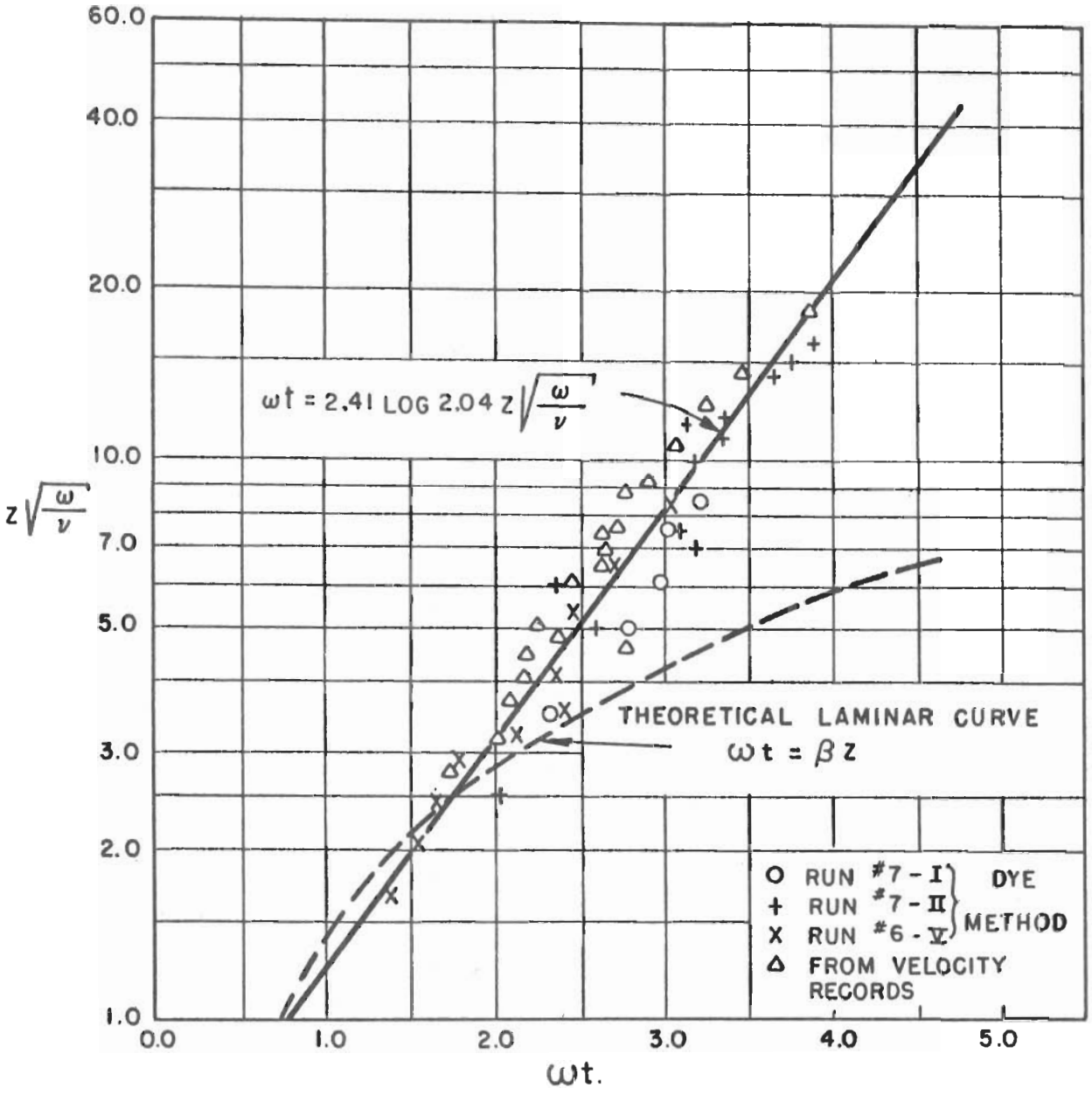

FIG. II PLOTTING OF EXPERIMENTAL DATA OF PHASE SHIFT MEASUREMENT (SMOOTH BOTTOM)

measurements were made with respect to the motion of the wall was readily taken from the record, figure 9(b). It was measured on the time scale and it was averaged out for a number of periods. A correction, though, of this average value was deemed necessary for the following reason. The acceleration in this type of flow is always ninety degrees different in phase from the velocity. Therefore, when the velocity approaches zero, the acceleration approaches its maximum absolute value. This results in the greatest distortion of the record at the region $u \cong 0$. As can be seen on the calibration record, figure (9a), although the motion of the instrument is in phase with the driving mechanism, the velocity curve goes through zero before the end of the stroke. This phase leading, which is due to acceleration, increases with increasing angular velocity ω .

For different frequencies of motion, this phase leading was measured on the calibrating record. In the actual measurements, it was reasonable to assume that the velocity records were leading by an equal angle and in order to obtain the true value of the phase shift, the measured time intervals had to be increased by the correction which corresponded to the angular velocity. It is interesting to note that the data obtained in this way (Table VI) checks very closely with that of the dye method (Figure 11). This not only proves that both methods are quite accurate, but also that the instrument is very reliable in measuring the phase shift. The main advantage in using the instrument for this purpose is that it is free from personal bias.

SUGGESTIONS FOR FURTHER INVESTIGATION

The present study covers only the case of the oscillatory turbulent boundary layer flow for the smooth case; the next step should be to investigate the case of a rough wall for two and three dimensional roughness. An expression similar to the one presented here might be derived which will describe the flow for the case of a rough wall. The three dimensional elements of roughness might be considered as behaving hydraulically similar to the bed grains at the sea bottom. Therefore, expressions for the hydrodynamic forces acting upon them can be derived. Applications of similar concepts as for the unidirectional flow may lead to the development of a theory governing the transportation of sediment by an oscillating flow. The theoretical results may be compared with actual measurement and the validity of the theory can thus be checked.

CONCLUSIONS

The flow near the bed in relatively deep water is essentially a shear flow and is attributed to the action of surface waves. The thin layer near the solid boundary within which shear flow occurs is called a boundary layer. Outside this layer the flow is potential and can be described by the irrotational theory of motion. At the interface, the water particles oscillate with a simple harmonic motion of an amplitude depending upon the characteristics of the surface waves and the depth of the water. The description of the flow in the boundary layer can be related to and deduced from the case of flow in the boundary layer

due to the oscillation of the solid boundary with a simple harmonic motion of the same characteristics.

Depending upon the amplitude and period of the motion and the viscosity of the water, the shear flow can be either laminar or turbulent. When in the case of an oscillating solid boundary the flow is laminar, it can be described by the Navier-Stoke's equation of motion

$$\frac{\partial u}{\partial t} = \nu \frac{\partial^2 u}{\partial z^2}$$

where ν is a constant. The distribution of velocities along the vertical is given by a solution of this equation of the form

$$u = u_o e^{-\beta z} \sin(\omega t - \beta z)$$

where $\beta \sqrt{\frac{\omega}{2\nu}}$

and u_o is the amplitude of the velocity of the oscillating wall.

The effective thickness of the boundary layer within which shear flow occurs was arbitrarily defined as the distance δ_1 from the solid boundary at which the amplitude of the velocity is reduced to one hundredth of the maximum value u_o. This thickness is

$$\delta_1 = 6.5\sqrt{\frac{\nu}{\omega}}$$

When the shear flow becomes turbulent, it can be described by the following two equations of motion:

a. $$\frac{\partial u}{\partial t} = \epsilon_v \frac{\partial^2 u}{\partial z^2}$$

b. $$\frac{\partial u}{\partial t} = \frac{\partial}{\partial z} \left(\epsilon_m \frac{\partial u}{\partial z} \right)$$

Where ϵ_v and ϵ_m are the coefficients of vorticity exchange and momentum exchange respectively.

In both cases, an assumption is made that the main flow velocity has a component in the x direction only, which at all distances from the bottom is a simple harmonic motion with the same period as the wall. The distribution of the velocity along the vertical can be given by a solution of equations a. and b. of the form

$$\frac{u}{u_o} = A \sin(\omega t - B)$$

A and B are functions of the distance z only. The function A has been determined experimentally and it was found to be $A = 0.428 \left(z\sqrt{\frac{\omega}{\nu}}\right)^{-0.65}$. From equation a, if this expression of A is introduced in the solution, it is deduced that

$$B = \sqrt{c(c-1)}\ \log_e K_2 \frac{z}{z_o} = 1.05\ \log_e K_2\ \frac{z}{z_o}$$

and

$$\epsilon_v = \frac{\omega z^2}{(1-2c)\sqrt{c(c-1)}} = 0.65\ \omega\ z^2$$

K_2 has been found experimentally to be equal to 3.14.

then $$B = 1.05\ \log_e\ 3.14\ \frac{z}{z_o} = 2.41\ \log_{10}\ 3.14\ \frac{z}{z_o}$$

The solution thus becomes

$$\frac{u}{u_o} = 0.360\ (\frac{z}{z_o})^{-0.65}\ \sin\ (\omega t - 2.41\ \log_{10}\ 3.14\ \frac{z}{z_o})$$

where distance of the reference level $z_o = 1.54\sqrt{\frac{\nu}{\omega}}$.

The distribution of the velocities as described from the above equation loses significance near the boundary. To describe the flow in this region, the introduction of a viscous sublayer is necessary in a similar manner as in the unidirectional flow.

From equation b, by determining again that

$$A = Kz^c = 0.428\ (\sqrt{\frac{\omega}{\nu}})^{-0.65}$$

and assuming that B is a logarithmic function of z, we deduce

$$B = \sqrt{c(c+1)}\ \log_e K_2\ z\sqrt{\frac{\omega}{\nu}}$$

and $$\epsilon_m = \frac{\omega z^2}{(2c+1)\sqrt{c(c+1)}}$$

The solution then takes the form

$$\frac{u}{u_o} = 0.360\ (\frac{z}{z_o})^{-0.65}\ \sin\ (\omega t - \sqrt{c(c+1)}\ \log_e K_z \frac{z}{z_o})$$

The phase shift function of this solution and the expression for the coefficient of momentum exchange ϵ_m have significance only when $c < -1$.

The experiment so far showed that $-1 < c < c$ which makes the validity of equation b questionable.

ACKNOWLEDGMENTS

The writer wishes to express his deep appreciation to Professor H. A. Einstein who suggested this problem to him and who offered a very material assistance to all its phases, and to Professor L. M. Grossman and P. L. Chambre for their keen interest and their valuable discussions.

He also expresses his gratitude to Dr. Huon Li for his help in the theoretical approach of the problem and his cooperation during the experimental work in dealing with electronic equipment, and to J. A. Harder under whose advice the velocity measuring instrument has been designed.

W. A. Hewitt, W. J. Ferguson and the staff of the Fluid Mechanics Laboratory contributed materially in the successful handling of the experimental equipment and their cooperation is gratefully acknowledged.

REFERENCES

1. Beach Erosion Board, Corps of Engineers, "A Summary of Theory of Oscillatory Waves", Technical Report No. 2, Washington: Government Printing Office (1942).

2. Boussinesq, J., "Theorie de l'Ecoulement Tourbillonnant et Tumultueux des Liquides", Paris: Gauthier-Villars et Fils, Imprimeurs-Libraires (1897), pp. 8-13.

3. Einstein, H. A. , "Bed-Load Function for Sediment Transportation in Open Channel Flows", U. S. Dept. of Agric., Soil Conservation Service Publication Tech. Bul. No. 1026 (1950).

4. Goldstein, S. , "Modern Developments in Fluid Dynamics", 1st Ed. Oxford: Clarendon Press (1938), Vol. I. pp. 191-233.

5. Kalinske, A. A., "Movement of Sediment as Bed-Load in Rivers", Trans. American Geophysic. Union., Vol.28 (1947) pp.615-20.

6. Lamb, H., "Hydrodynamics", 6th Edition, New York: Dover Publications (1945), p. 619.

7. Li, Huon, "Stability of Oscillatory Laminar Flow Along a Wall", Tech. Memo. No. 47, Beach Erosion Board, Corps of Engineers, Aug. 1954.

8. Li, Huon, "On the Measurement of Pressure Fluctuations at the Smooth Boundary of an Incompressible Turbulent Flow", U. C. IER, Series No. 65, Issue No. 1, December 1954.

9. Manohar, Madhav, "Mechanics of Bottom Sediment Movement Due to Wave Action", Tech. Memo No. 75, Beach Erosion Board, Corps of Engineers, June 1955.

10. Prandtl, L., "Essentials of Fluid Dynamics", Blackie & Sons, Lmtd., London, 1952, pp. 11-129.

11. Wiegel, R. L. and Johnson, J. W., "Elements of Wave Theory", in J. W. Johnson (edit.) Coastal Engineering, Vol. 1, Berkeley, California Council on Wave Research, Univ. of California, (1950), pp. 5-21.

APPENDIX

Tables of Experimental Data

TABLE Ia

Experimental Data
Phase Shift Measurement
Rough Bottom: $\frac{3}{4}$" Diam. Half Round Wooden Strips

I	$\nu = 1.06 \times 10^{-5} ft^2/sec.$				II $\nu = 1.06 \times 10^{-5} ft^2/sec.$			
z ft.	ω rad. sec.	$z\sqrt{\frac{\omega}{\nu}}$	t sec.	ωt	ω rad. sec.	$z\sqrt{\frac{\omega}{\nu}}$	t sec.	ωt
0.0098	0.392	1.88	2.84	1.01	0.402	1.90	2.30	0.93
0.0196	0.383	3.71	3.40	1.30	0.402	3.80	2.96	1.18
0.0295	0.396	5.48	4.86	1.79	0.394	5.70	3.62	1.42
0.0393	0.338	7.00	5.72	1.93	0.389	7.50	4.66	1.81
0.0491	0.340	8.77	7.35	2.50	0.384	9.35	5.82	2.24
0.0590	0.415	11.60	7.72	3.18	0.379	11.05	7.00	2.65
0.0688	0.400	13.35	8.57	3.43	0.374	12.90	7.42	2.77
0.0781	0.386	14.90	9.10	3.51	0.360	14.40	9.44	3.40
0.0885	0.378	16.70	9.95	3.76	0.386	16.90	9.23	3.56
0.0985	0.367	18.30	10.54	3.87	0.382	18.70	9.85	3.76

TABLE Ib

Experimental Data
Phase Shift Measurement
Rough Bottom $\frac{3}{4}$" Diam. Half Round Wooden Strips

z ft.	$\nu = 1.06 \times 10^{-5}$ ft^2/sec							
	III				IV			
	ω r/sec	$z\sqrt{\frac{\omega}{\nu}}$	t sec	ωt	ω r/sec	$z\sqrt{\frac{\omega}{\nu}}$	t sec	ωt
0.0098					0.405	1.93	2.10	0.85
0.0196	0.375	3.68	3.42	1.28	0.407	3.84	3.06	1.24
0.0295	0.366	5.46	3.87	1.42	0.407	5.77	4.21	1.71
0.0393	0.364	7.28	5.05	1.84	0.380	7.41	5.64	2.14
0.0491	0.353	8.95	7.07	2.50	0.388	9.40	6.12	2.37
0.0590	0.392	11.30	7.57	2.97	0.392	11.30	7.40	2.90
0.0688	0.386	13.10	8.40	3.24	0.388	13.15	8.07	3.14
0.0781	0.382	14.80	9.28	3.54	0.392	15.00	8.87	3.48
0.0885	0.374	16.60	9.80	3.66	0.396	17.10	9.48	3.75
0.0985	0.373	18.40	10.31	3.84	0.407	19.30	10.16	4.13

TABLE II

Experimental Data
Phase Shift Measurement
Smooth Bottom

z ft	$\nu = 1.20 \times 10^{-5}$ ft^2/sec							
	I				II			
	ω r/sec	$z\sqrt{\frac{\omega}{\nu}}$	t sec	ωt	ω r/sec	$z\sqrt{\frac{\omega}{\nu}}$	t sec	ωt
0.010	1.57	3.62	0.70	1.57	1.01	2.90	1.10	1.10
0.015	1.57	5.43	0.90	1.41	0.99	4.32	1.60	1.60
0.020	1.57	7.24	1.00	1.57	1.01	5.80	1.83	1.86
0.025	1.57	9.05	1.10	1.73	0.99	7.20	2.38	2.37
0.030	1.57	10.90	1.60	2.51	1.01	8.70	2.38	2.41
0.035	1.57	12.70	1.70	2.67	1.01	10.15	2.54	2.58
0.040	1.57	14.50	2.00	3.14	1.01	11.60	2.98	3.02
0.045	1.57	16.30	2.22	3.49	0.99	12.95	3.01	3.00
0.050	1.57	18.10	2.20	3.45				
0.055	1.57	19.90	2.70	4.24				
0.060	1.57	21.70	2.80	4.40				

TABLE III

Velocity Measurement
Calibration Data

T sec	ω r/sec	U ft°/s	y mm
2.51	2.50	0.625	16.50
2.61	2.40	0.599	14.90
2.74	2.29	0.572	13.70
2.91	2.16	0.540	12.00
3.25	1.95	0.483	9.90
3.30	1.90	0.475	9.60
3.50	1.79	0.443	8.30
3.87	1.62	0.405	6.90
4.40	1.43	0.356	5.50
4.43	1.42	0.354	5.60
5.48	1.15	0.286	3.50
6.95	0.95	0.226	2.50

TABLE IVa

Velocity Measurement Data

Run: 1 (#4 - I)

a_b' = 1.0 ft. d' = 2.0 ft.

T = 2.76 sec. ω = 2.275 rad/sec.

U_o = 2.275 ft/sec.

ν = 1.06 x 10^{-5} ft^2/sec.

z ft	$z\sqrt{\frac{\omega}{\nu}}$	y mm.	U ft/sec	U/U_o
0.006	2.78	10.50	0.500	0.220
0.007	3.24	8.92	0.456	0.205
0.008	3.70	6.67	0.395	0.174
0.009	4.16	4.91	0.323	0.142
0.011	5.10	4.35	0.309	0.136
0.014	6.49	2.61	0.234	0.102
0.015	6.95	2.56	0.232	0.101
0.019	8.80	2.30	0.219	0.096
0.023	10.60	1.50	0.125	0.055

TABLE IVb

Velocity Measurement Data

Run: 2 (#4 - II)

a_b' = 1.50 ft. d' = 3.00 ft.

T = 3.53 sec. ω = 1.78 rad/sec.

U_o = 2.67 ft/sec. ν = 1.06 x 10^{-5} $ft^2/sec.$

z ft	$z\sqrt{\frac{\omega}{\nu}}$	y mm.	U ft/sec	U/U_o
0.010	4.10	9.60	0.476	0.179
0.011	4.51	8.17	0.434	0.163
0.012	4.92	8.08	0.432	0.162
0.013	5.33	6.40	0.381	0.143
0.014	5.74	5.65	0.354	0.133
0.015	6.15	5.50	0.352	0.132
0.016	6.56	5.35	0.346	0.130
0.017	6.97	5.07	0.335	0.126
0.018	7.38	4.67	0.322	0.120
0.019	7.79	4.22	0.304	0.114
0.020	8.20	4.00	0.296	0.111
0.021	8.61	3.90	0.292	0.109
0.022	9.02	3.59	0.279	0.104
0.023	9.43	3.16	0.260	0.098
0.024	9.84	3.20	0.262	0.098
0.025	10.23	3.08	0.257	0.096
0.026	10.66	2.70	0.239	0.089
0.027	11.07	2.64	0.237	0.088
0.029	11.89	2.50	0.230	0.086
0.031	12.71	2.31	0.220	0.082
0.033	13.53	2.00	0.204	0.077
0.035	14.35	1.87	0.196	0.073
0.040	16.40	1.50	0.174	0.065

TABLE IVc

Velocity Measurement Data

Run: 3 (#4 - III)

a_b' = 1.5 ft. d' = 3.0 ft.

T = 2.68 sec. ω = 2.34 rad/sec.

U_o = 3.52 ft/sec. ν = 1.06 x 10^{-5} $ft^2/sec.$

z ft	$z\sqrt{\frac{\omega}{\nu}}$	y mm.	U ft/sec.	U/U_o
0.001	5.17	15.02	0.604	0.171
0.012	5.64	13.75	0.528	0.150
0.013	6.11	11.70	0.526	0.149
0.014	6.58	10.70	0.503	0.143
0.016	7.52	9.20	0.464	0.132
0.017	7.99	8.05	0.425	0.121
0.018	8.46	7.55	0.416	0.118
0.019	8.93	7.40	0.411	0.117
0.020	9.40	6.45	0.382	0.108
0.021	9.87	6.10	0.371	0.105
0.022	10.34	5.40	0.348	0.099
0.023	10.31	5.15	0.336	0.095
0.025	11.75	4.55	0.318	0.090
0.027	12.69	3.78	0.286	0.081
0.031	14.57	3.42	0.272	0.077
0.033	15.51	3.18	0.262	0.074
0.035	16.45	2.71	0.240	0.068
0.040	18.80	2.22	0.215	0.061

TABLE V

Phase Shift Measurement
Dye Method

	z ft.	ω rad. sec.	$z\sqrt{\frac{\omega}{\nu}}$	t sec.	ωt
Run: 1	0.005	1.79	2.055	0.864	1.55
(#6 - V)	0.006	1.79	2.466	0.936	1.68
	0.007	1.79	2.877	0.983	1.76
	0.008	1.79	3.288	1.174	2.10
	0.010	1.79	4.110	1.303	2.33
	0.013	1.79	5.383	1.345	2.41
	0.016	1.79	6.576	1.495	2.68
	0.020	1.79	8.220	1.680	3.02
Run: 2	0.005	2.60	2.50	0.800	2.08
(#7 - I)	0.007	2.60	3.50	0.890	2.31
	0.010	2.60	5.00	1.070	2.78
	0.012	2.60	6.00	1.135	2.95
	0.015	2.60	7.50	1.152	3.00
	0.017	2.60	8.50	1.230	3.20
Run: 3	0.005	2.59	2.50	0.810	2.02
(#7 - II)	0.010	2.59	5.00	1.000	2.59
	0.014	2.59	7.00	1.260	3.16
	0.017	2.59	8.50	1.145	2.85
	0.022	2.59	11.00	1.290	3.32
	0.025	2.59	12.50	1.540	3.84
	0.030	2.59	15.00	1.500	3.74
	0.033	2.59	16.50	1.560	3.89

TABLE VI

Phase Shift Measurement
From the Velocity Records

	z ft.	ω rad. sec.	$z\sqrt{\frac{\omega}{\nu}}$	t sec.	ωt
Run: I	0.006	2.28	2.78	0.765	1.74
	0.007	2.28	3.24	0.890	2.02
	0.008	2.28	3.70	0.920	2.09
	0.009	2.28	4.17	1.010	2.31
	0.010	2.28	4.63	1.210	2.41
Run: II	0.010	1.78	4.10	1.213	2.16
	0.011	1.78	4.51	1.224	2.18
	0.012	1.78	4.92	1.343	2.39
	0.015	1.78	6.15	1.365	2.43
	0.016	1.78	6.56	1.475	2.62
	0.019	1.78	7.79	1.530	2.72
	0.023	1.78	9.43	1.625	2.89
	0.031	1.78	12.71	1.834	3.27
Run: III	0.011	2.34	5.17	0.957	2.24
	0.013	2.34	6.11	1.054	2.47
	0.015	2.34	7.05	1.130	2.65
	0.019	2.34	8.93	1.177	2.75
	0.023	2.34	10.81	1.309	3.06
	0.031	2.34	14.57	1.489	3.48
	01040	2.34	18.80	1.645	3.85